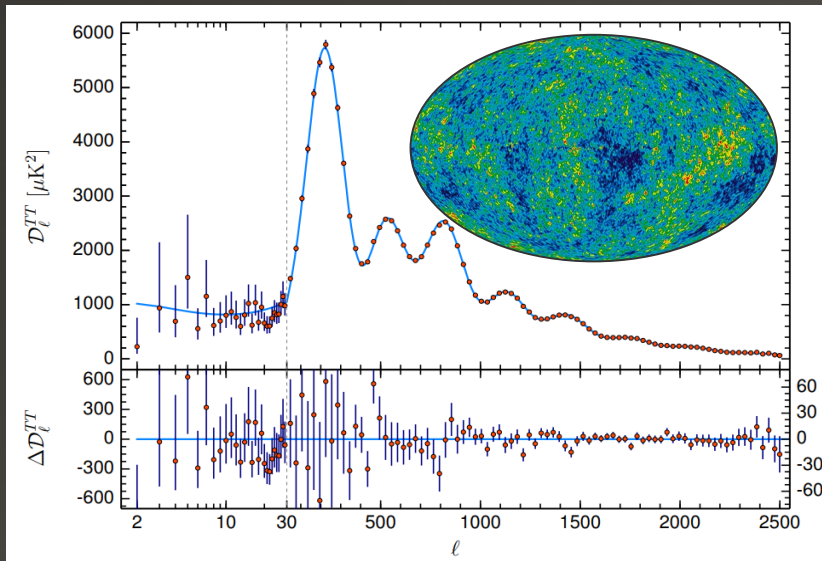


Novel Directions in Dark Matter Direct Detection

CARLOS BLANCO

The Glaring Problem: Dark Matter (DM)

Cosmic Microwave Background
cold non-interacting fluid



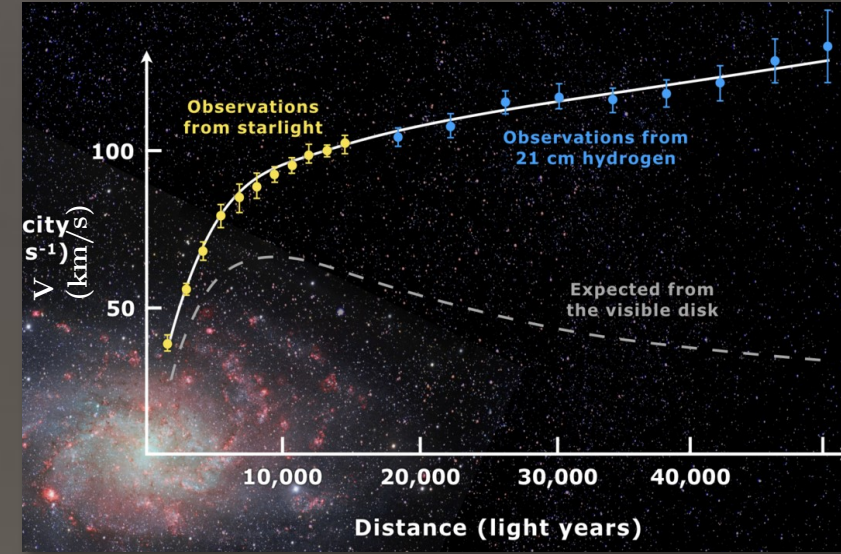
ESA and the Planck Collaboration 2020

Bullet cluster
dark and visible components separate



X-ray: NASA/CXC/CfA/M.Markevitch et al.;
Optical: NASA/STScI; D.Clowe et al.;
Lensing Map: NASA/STScI; D.Clowe et al.

Galactic rotation curves
invisible gravitating mass



Corbelli & Salucci, MNRAS 1999
Bosma, Astronomical Journal, 1989

“...we must *delve deep...* and *search wide*, to explore as much motivated DM parameter space as possible.”
Report of the Topical Group on Particle Dark Matter for Snowmass, arXiv:2209.07426.

Our dark matter halo



Image credit: ESO/L Calçada

We are here.

Local dark matter density

$$\rho_{\text{DM}} = 0.4 \text{ GeV}/\text{cm}^3$$

Local dark matter velocity

$$\langle v_{\text{DM}} \rangle \approx 300 \text{ km/s}$$

Lighter masses \rightarrow more particles

$$n_{\text{DM}} = \rho_{\text{DM}}/m_{\text{DM}}$$

More particles \rightarrow larger fluxes

$$\phi_{\text{DM}} \sim v_{\text{DM}} n_{\text{DM}}$$

What We Don't Know

Go After the Bare Minimum

Mass: How heavy and how many?

Coupling: How does it interact?

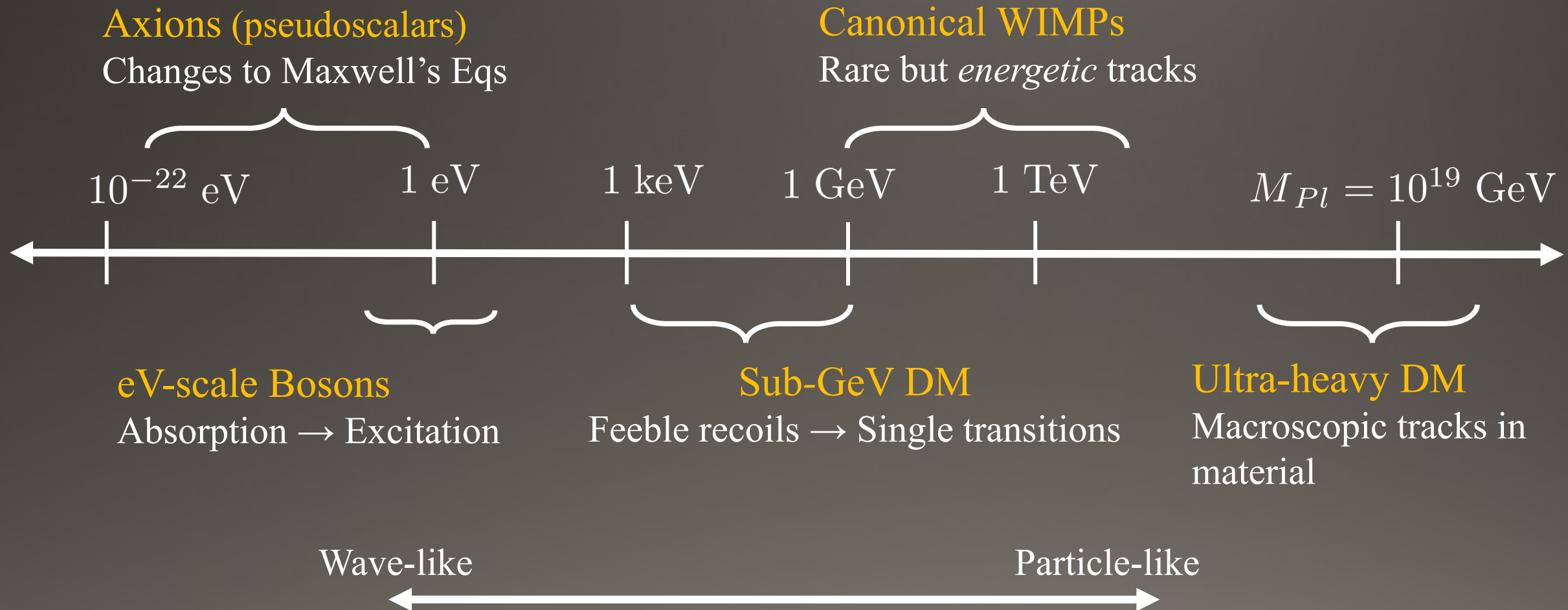
Production: How is it made?

The Method:

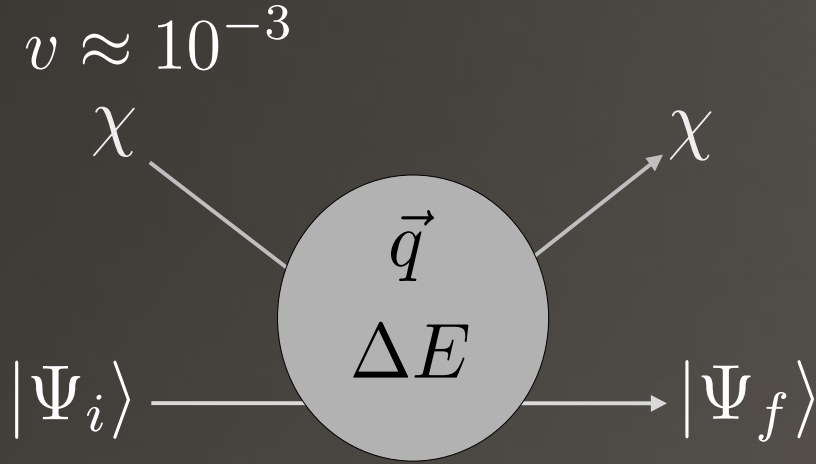
Bring together particle physics, condensed matter, chemistry, and astrophysics.

In brief, an *interdisciplinary* approach to the search for dark matter.

Mass Range & Detection Methods



How to Read These Plots

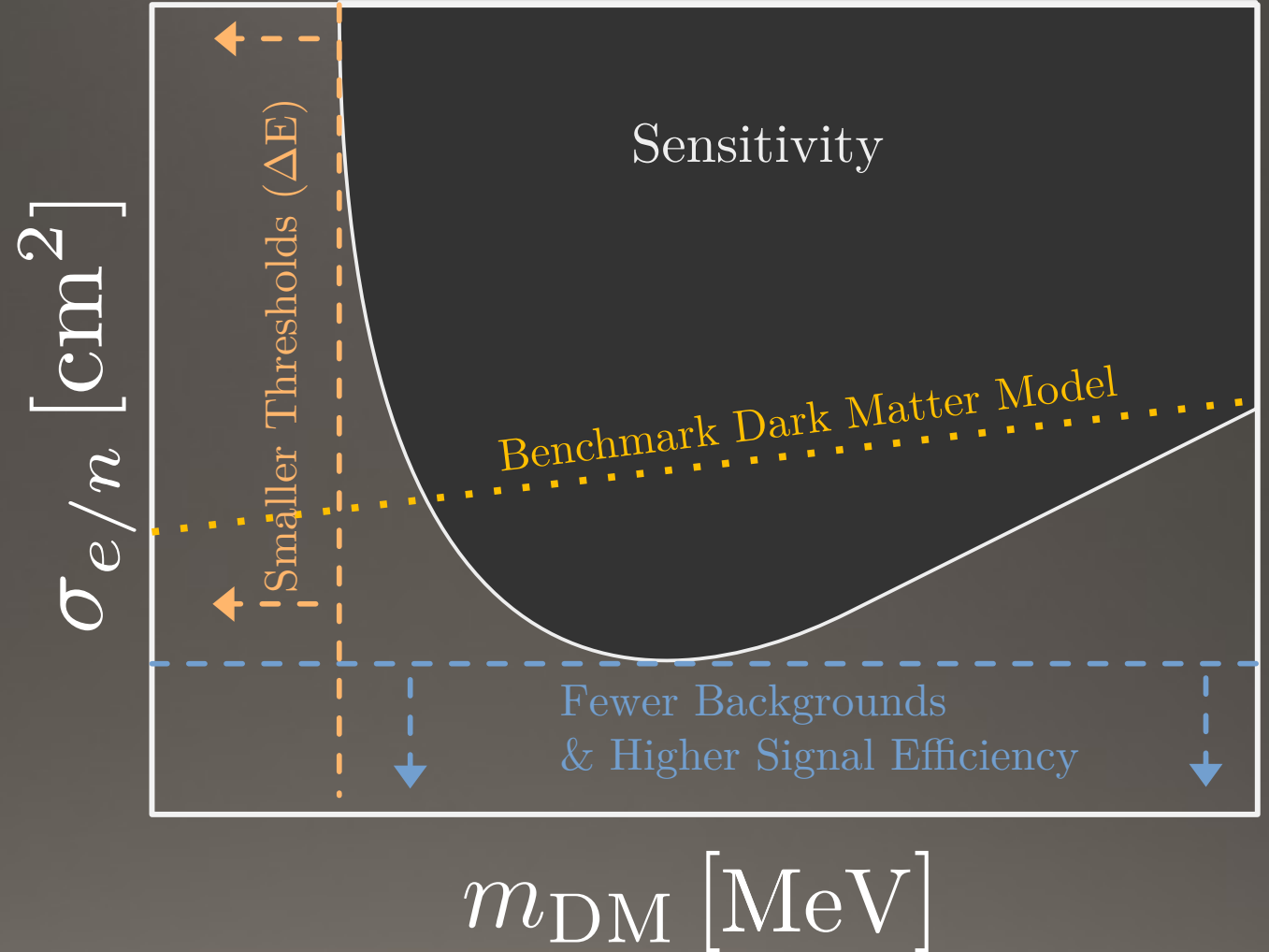


Energy Budget

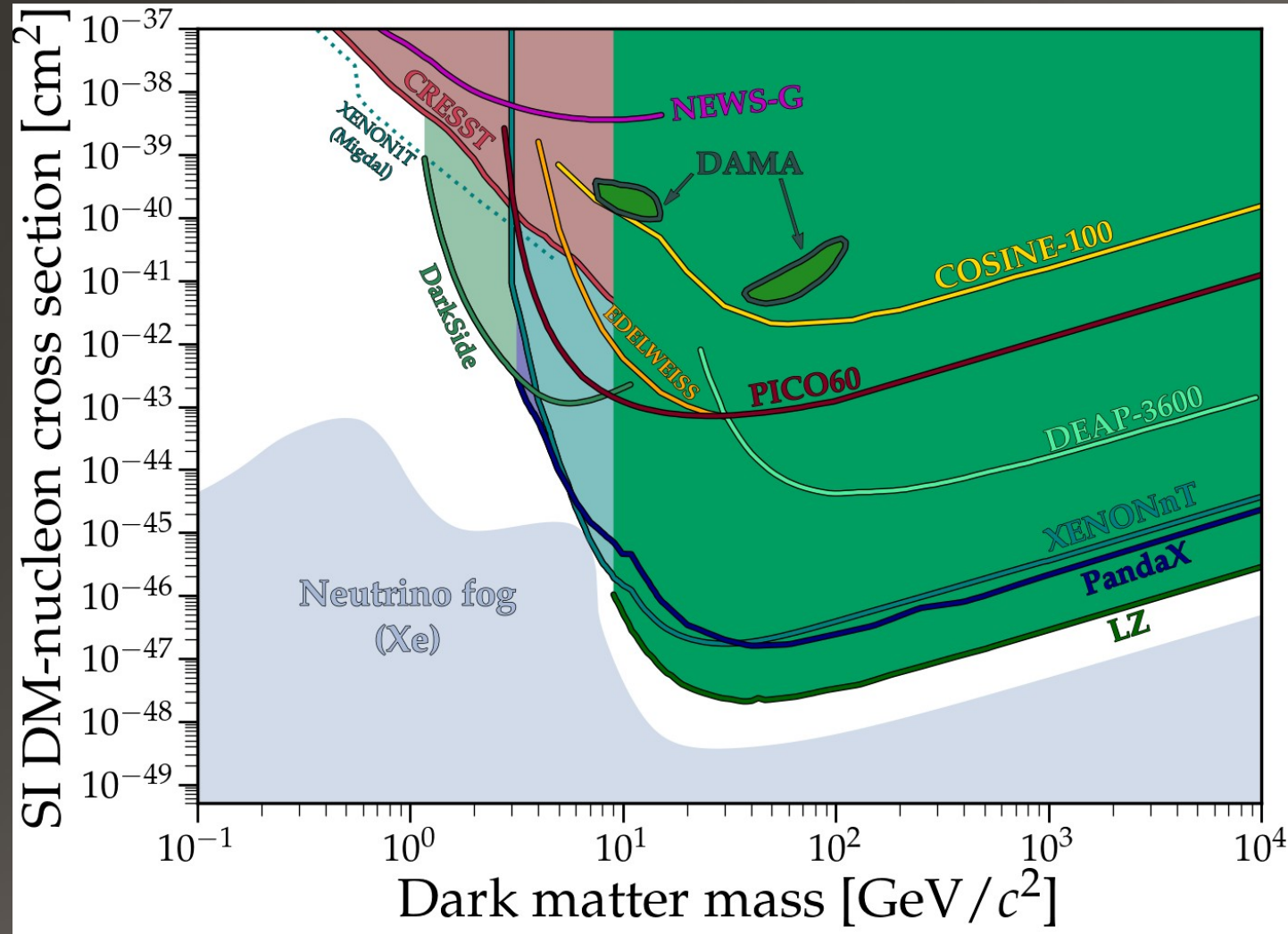
$$\Delta E \sim v^2 m_\chi \approx \mathcal{O}(\text{eV}) \left(\frac{m_\chi}{1 \text{ MeV}} \right)$$

Momentum Budget

$$q \sim v m_\chi \approx \mathcal{O}(\text{keV}) \left(\frac{m_\chi}{1 \text{ MeV}} \right)$$



Nucleon Scattering



Plot: Ciaran O'Hare - github.com/cajohare/DirectDetectionPlots
See e.g. [arXiv:2410.17036](https://arxiv.org/abs/2410.17036) & [2406.01705](https://arxiv.org/abs/2406.01705) and refs therein.

Noble Fluid-Based

- XENON - Xe
- PandaX - Xe
- LZ - Xe
- DarkSide - Ar
- DEAP-3600 - Ar
- NEWS-G (gas) – NH₄ (H, He, Ne)

Crystal Scintillator

- COSINE-100 - NaI (Ti)
- CRESST – CaWO₄

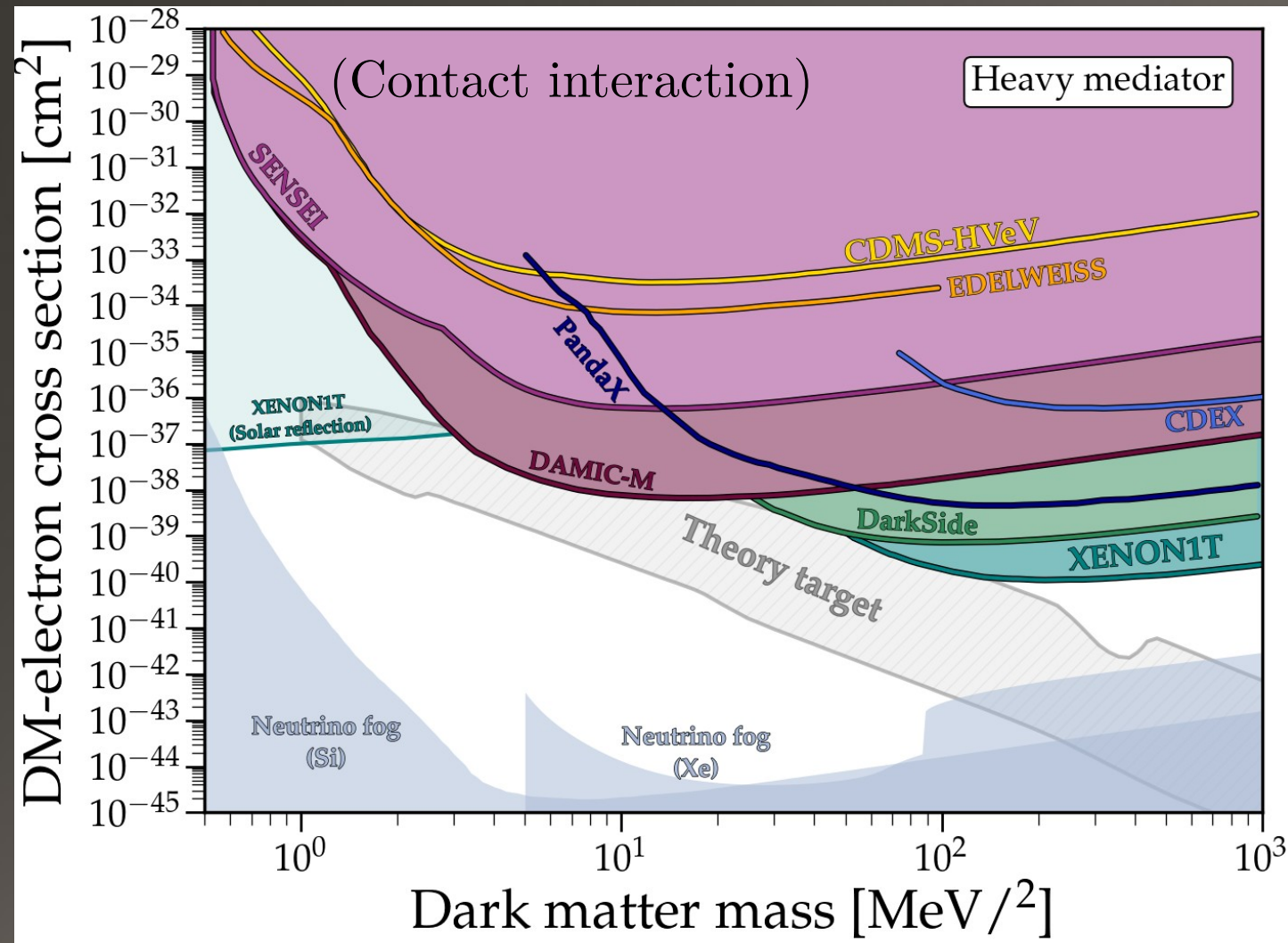
Bubble Chamber

- PICO60 - C₃F₈

Bolometers

- CRESST – CaWO₄
- EDELWEISS - Ge

Electron Recoil



Silicon CCDs

- SENSEI
- DAMIC-M

Liquid Noble Gases

- XENON - Xe
- PandaX - Xe
- Darkside - Ar

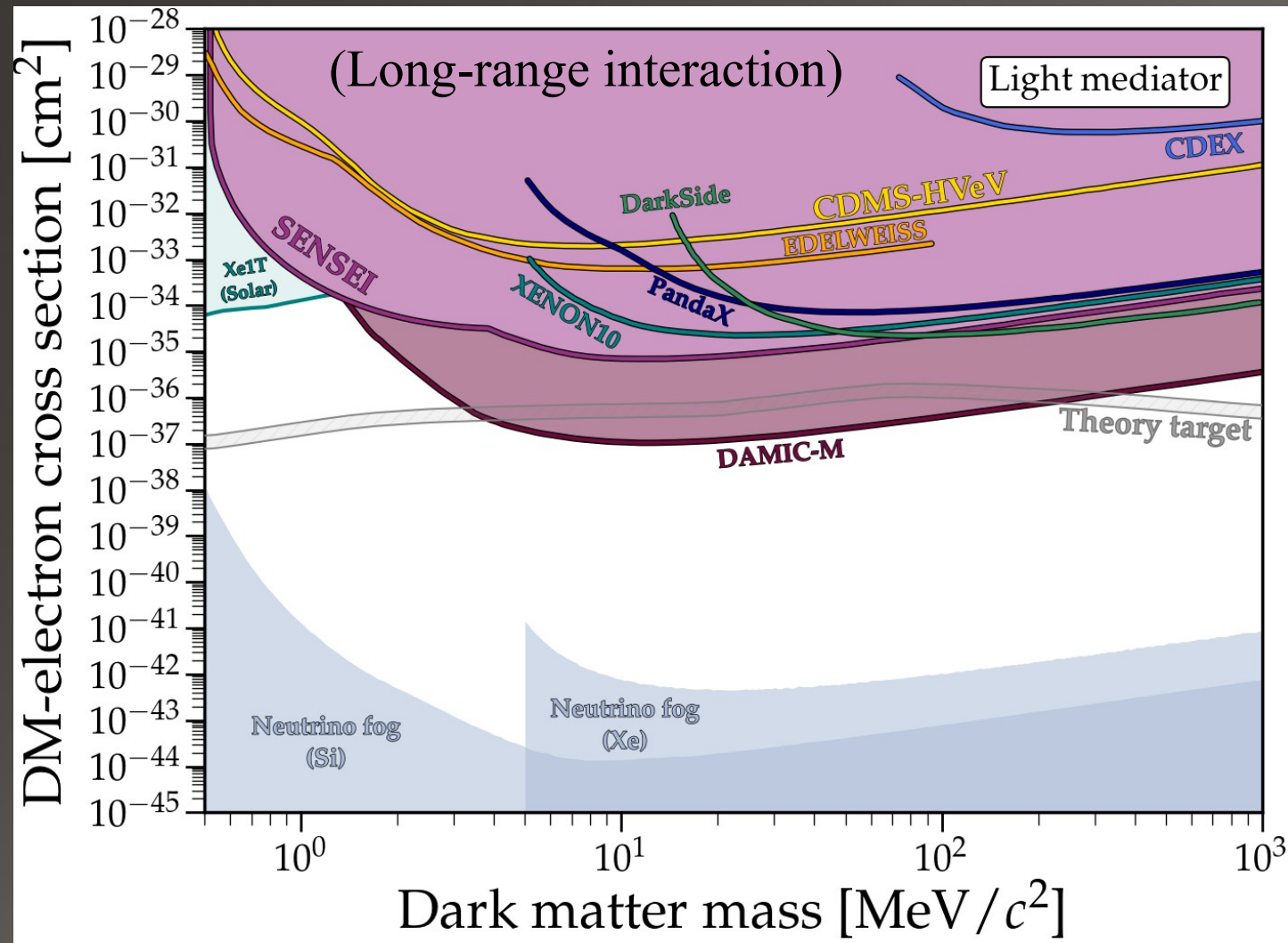
Bolometers

- EDLEWEISS - Ge
- CDMS – Ge & Si

Theory Targets

- ELDER/SIMP – Freeze out

Electron Recoil



Silicon CCDs

- SENSEI
- DAMIC-M

Liquid Noble Gases

- XENON - Xe
- PandaX - Xe
- Darkside - Ar

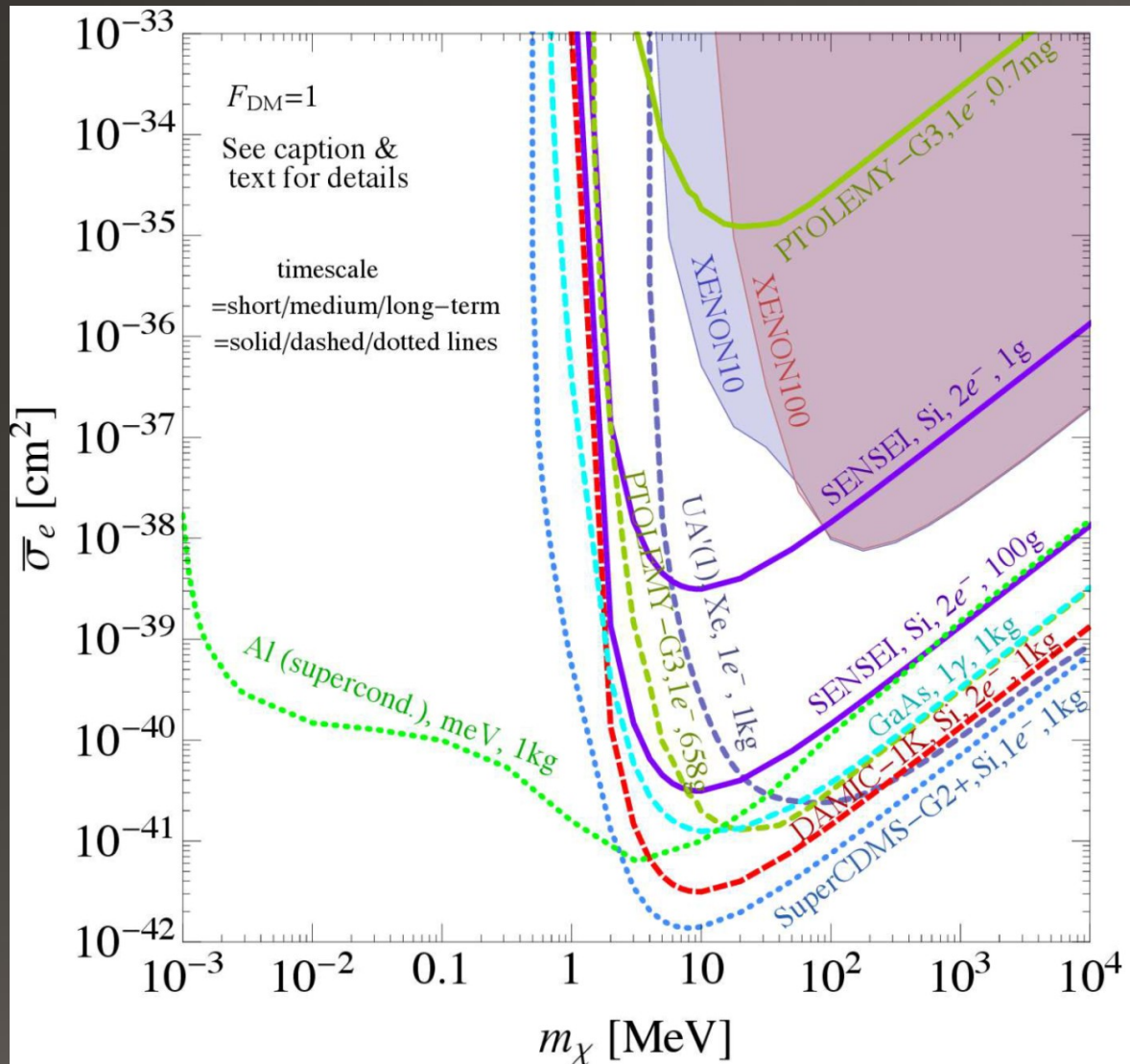
Bolometers

- EDELWEISS - Ge
- CDMS - Ge & Si

Theory Targets

- Freeze-in

The Field in Context



Many materials are proposed to probe the sub-GeV Space

In 2017:

Short term (2 years)



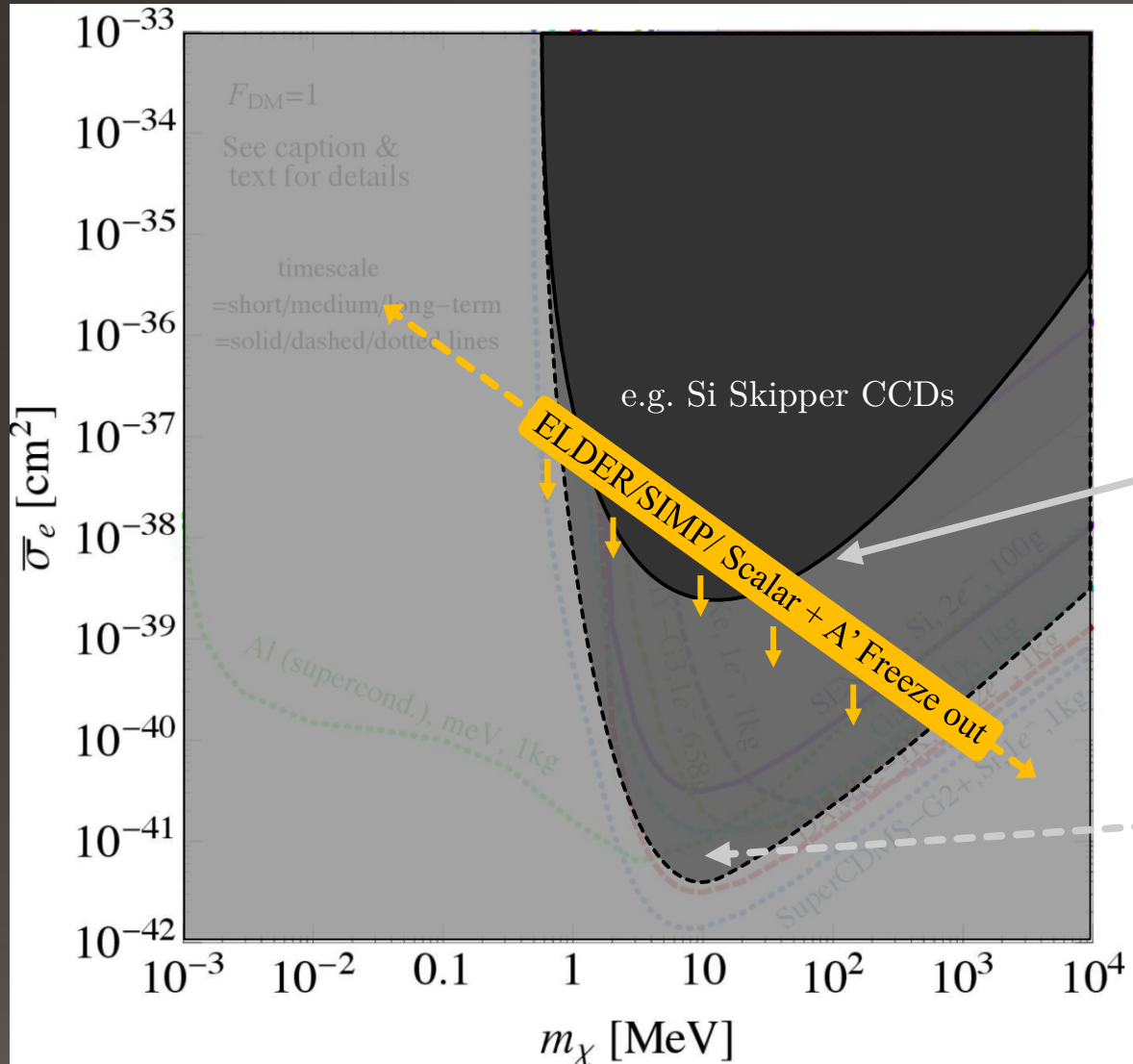
Medium term (2-5 years)



Long term



Outlook and Potential Reach



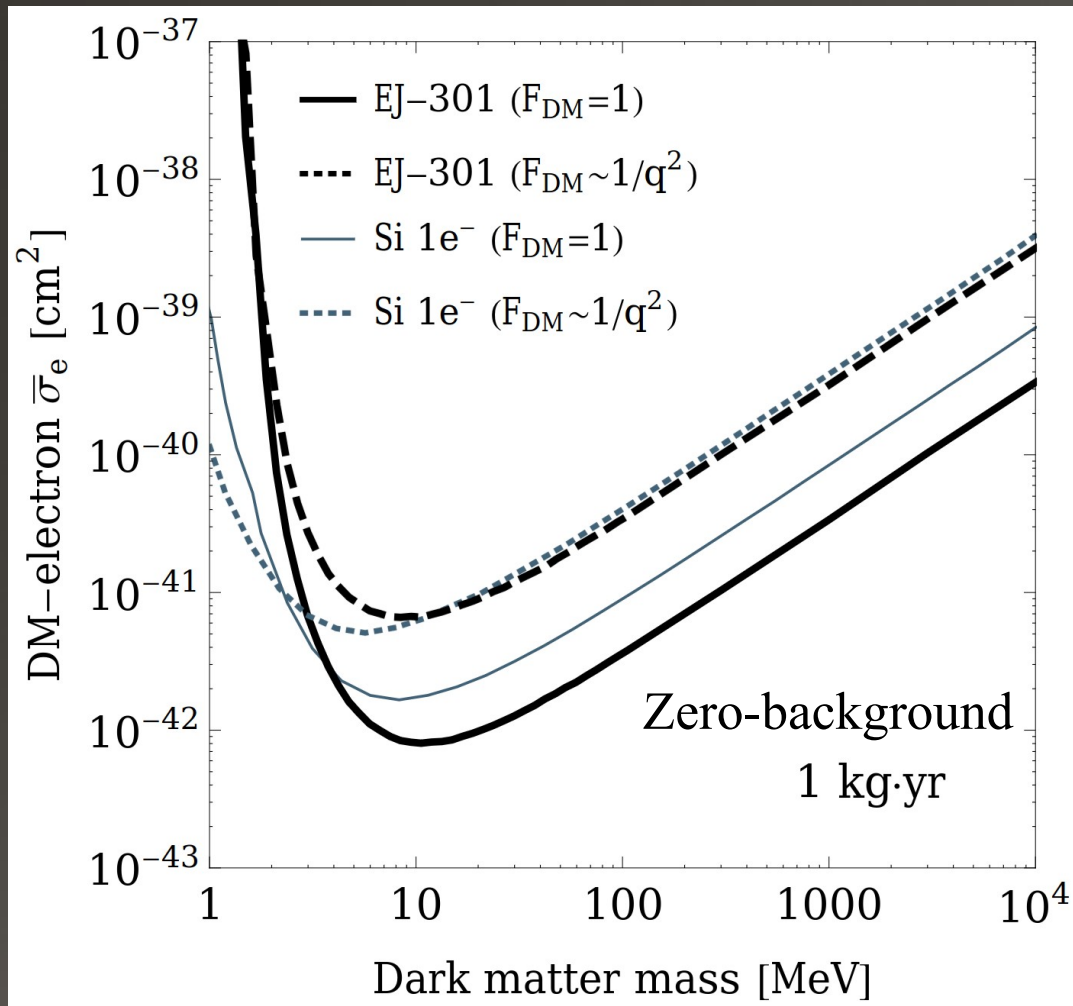
Present day:

Experimental results

Zero-background projection

Outlook and Potential Reach

[CB, Collar, Kahn, Lillard: 1912.02822]



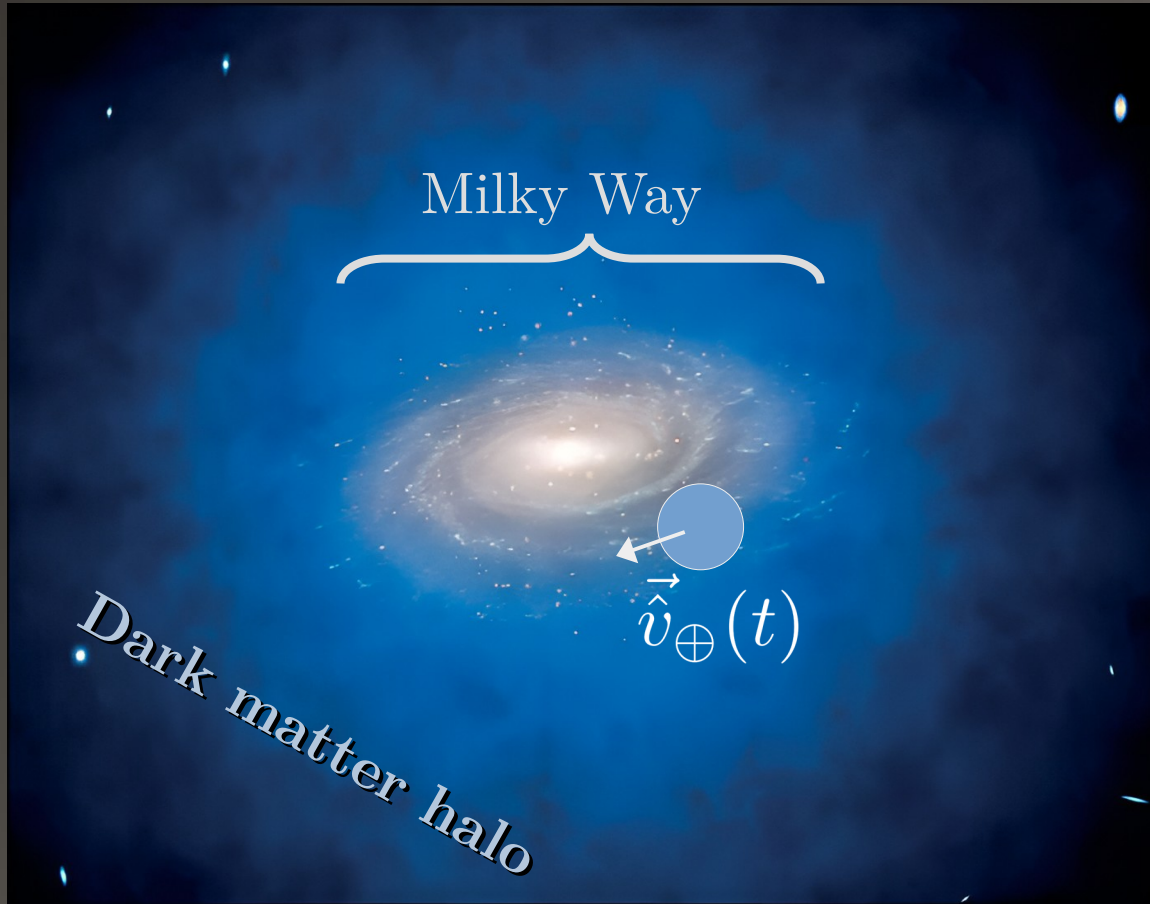
The obstacle

Backgrounds

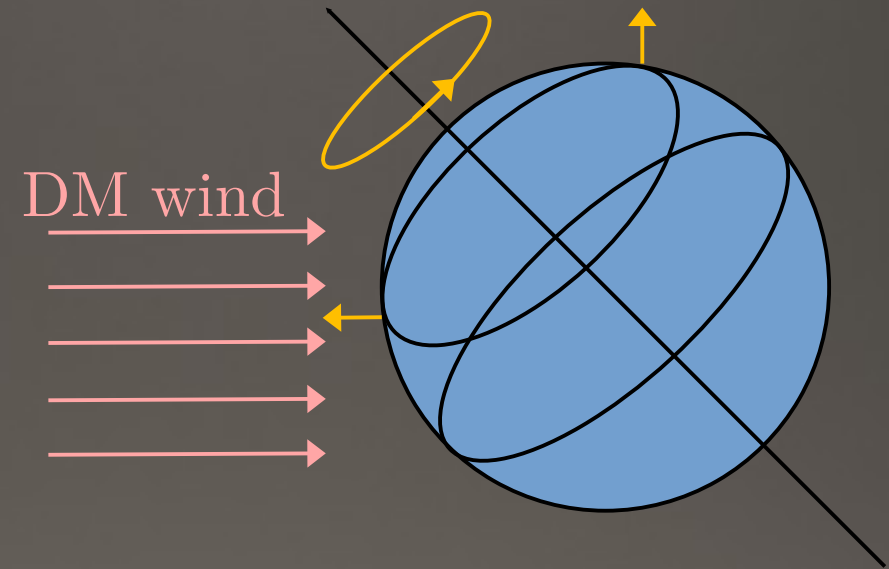
4 orders of magnitude of potential reach awaiting

Pound (kg) for Pound (kg) molecules produce about as much signal as e.g. Si.

Directional Detection

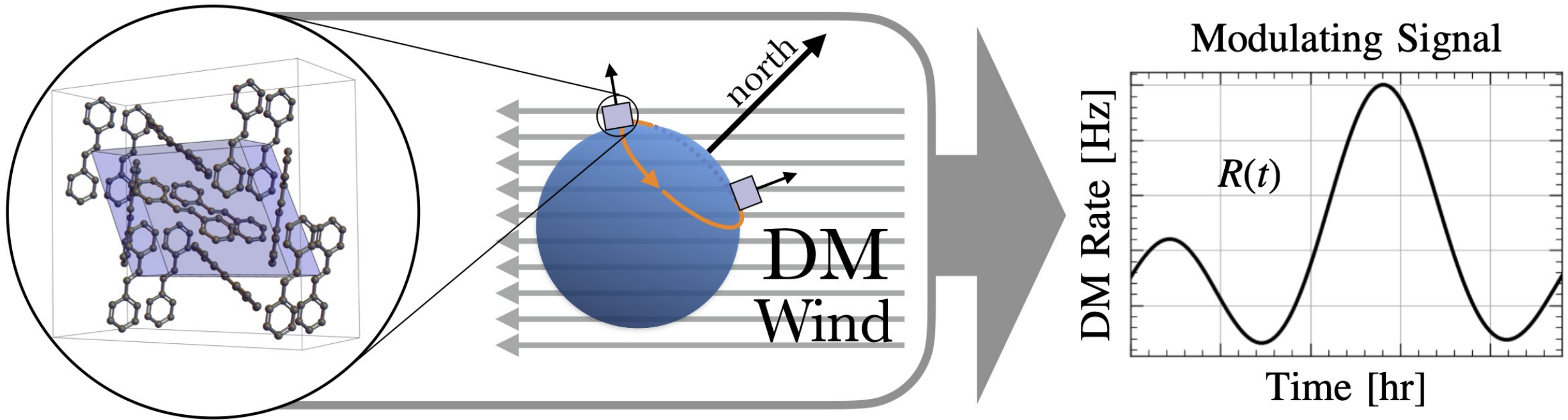


Effective dark matter “wind” from relative motion



Change in relative orientation between detector and dark matter wind leads to *daily modulation*

Towards a Directional Detector

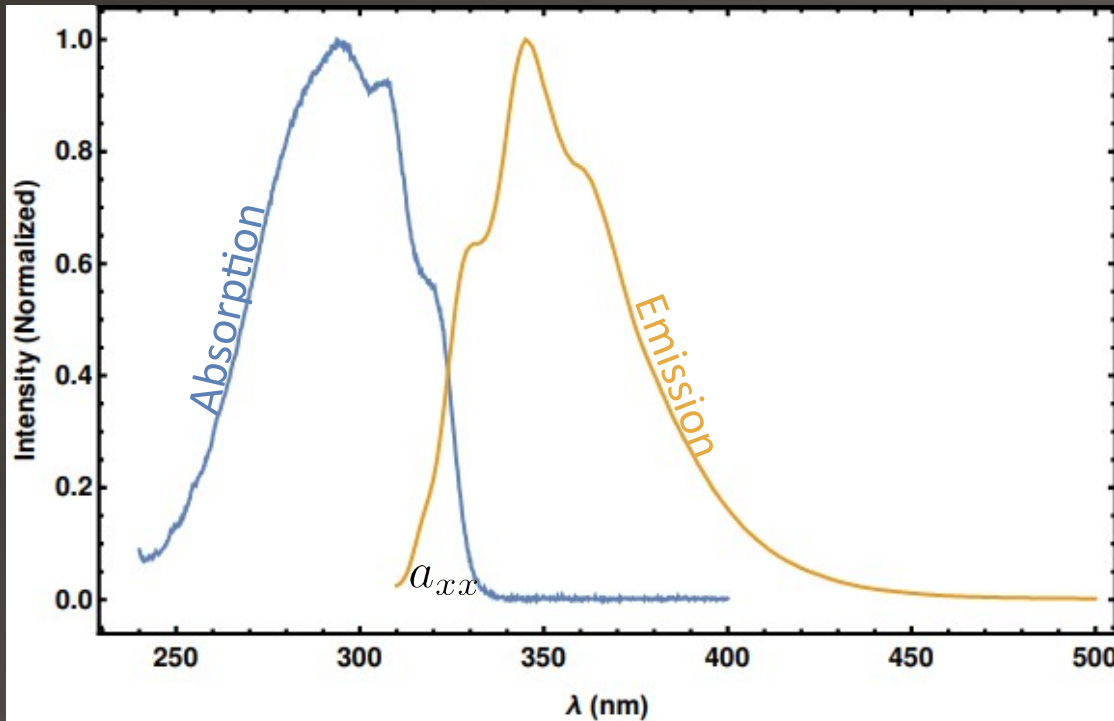


Modulating signals improve sensitivity by about two orders of magnitude and provide the potential for discovery.

Fluorescence with DM

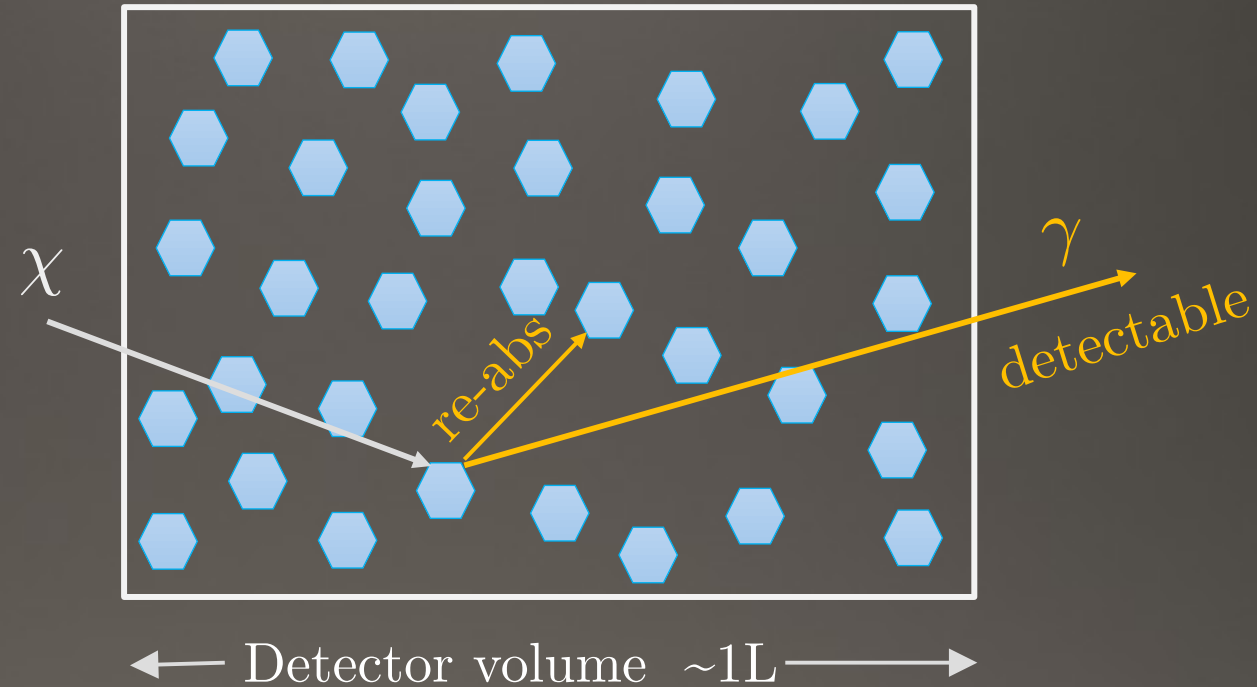
fluorescence spectra

Absorption/emission Probability



Decreasing energy (E) \rightarrow

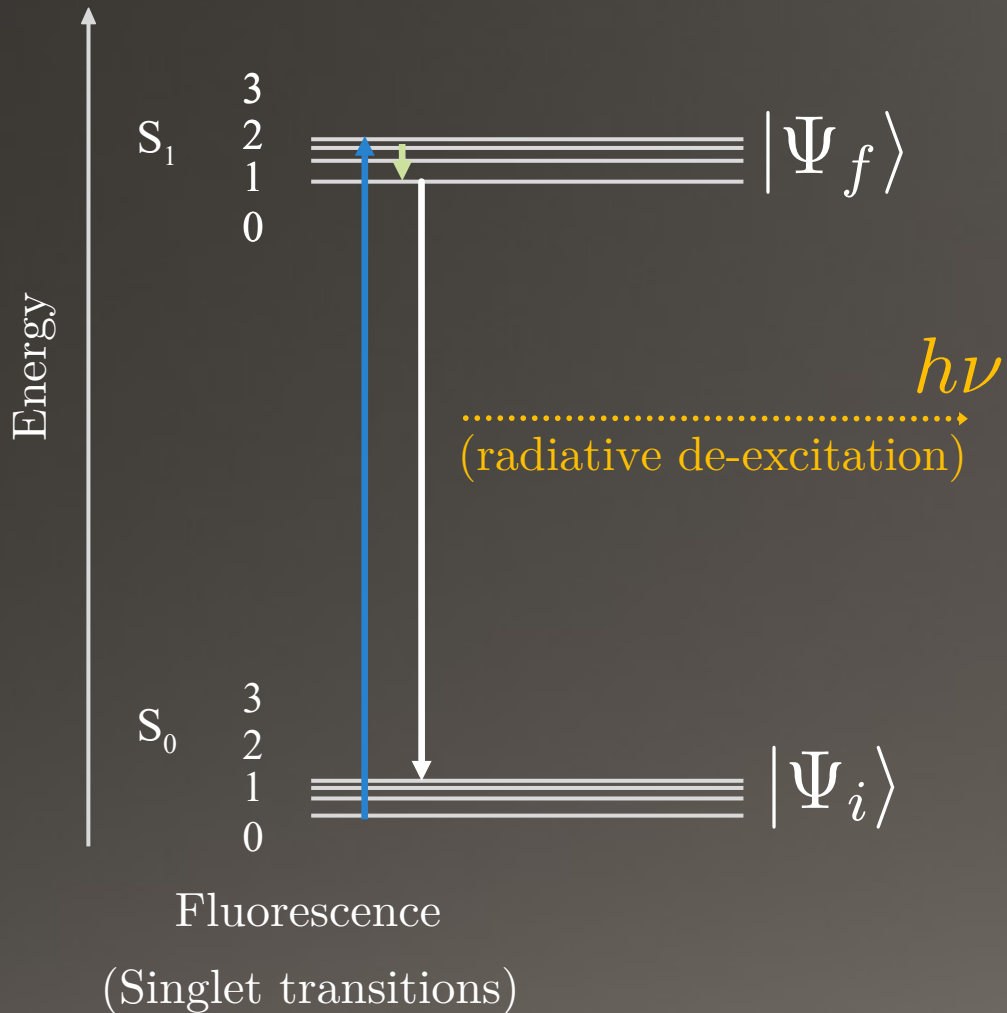
⬡: Chromophore:



Probability for the photon to free stream

$$\Phi_{\text{FB}} \sim (1 - a_{xx}) \quad \text{e.g. molecular crystals: } \Phi_{\text{FB}} \approx 65\%$$

Luminescent Detectors



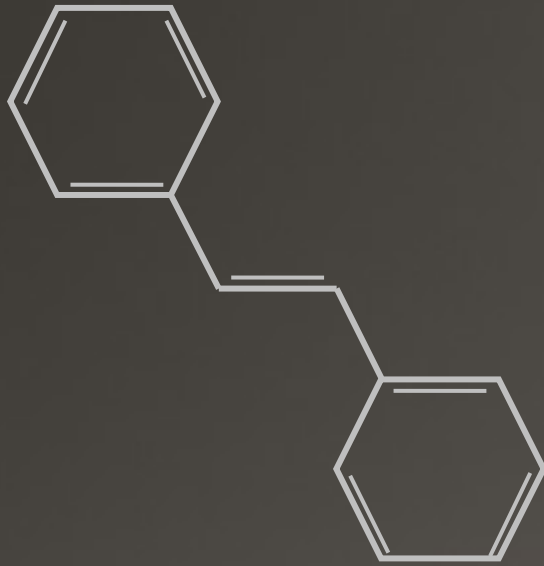
Energy Scale	Momentum Scale
$\Delta E \approx \mathcal{O}(\text{eV})$	$q \sim \alpha m_e \approx \mathcal{O}(\text{keV})$

Disambiguation*

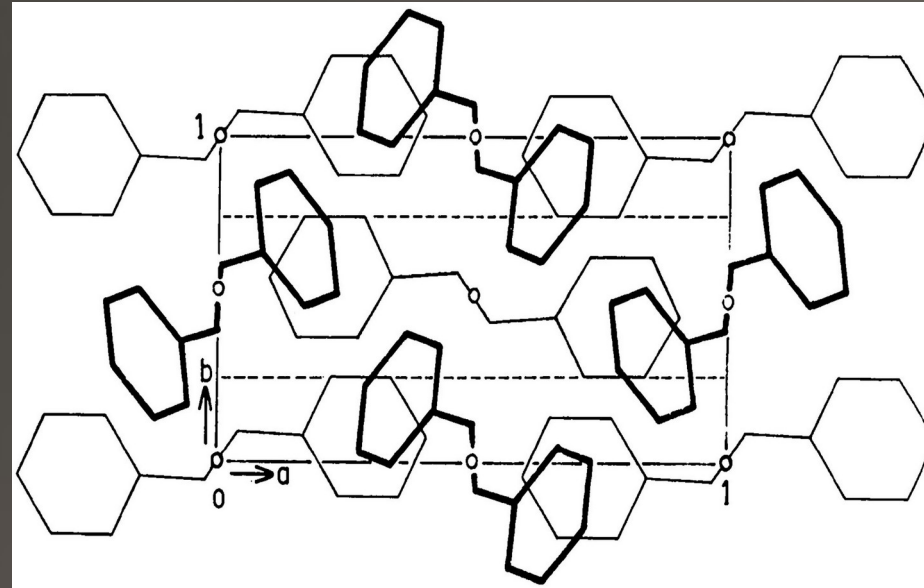
Scintillation: Initial $\mathcal{O}(\text{keV})$ recoil produces *many* ionized/excited states. These quickly deexcite, producing photons.

Fluorescence: Initial $\mathcal{O}(\text{eV})$ recoil produces *single* excited state, which deexcites, producing single photon.

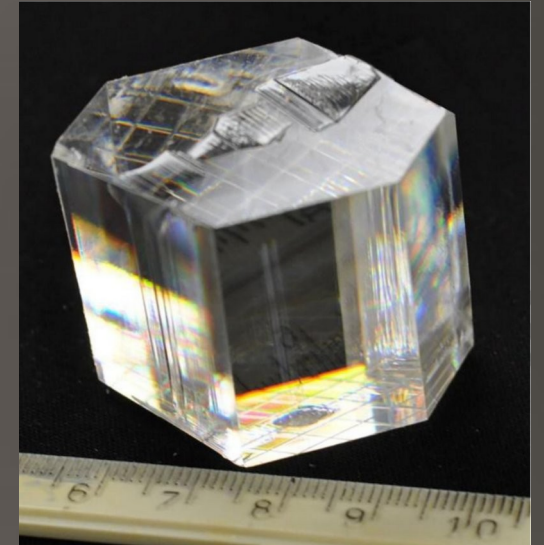
First Target Candidate: Trans-Stilbene



De-localized and planar network of double bonds



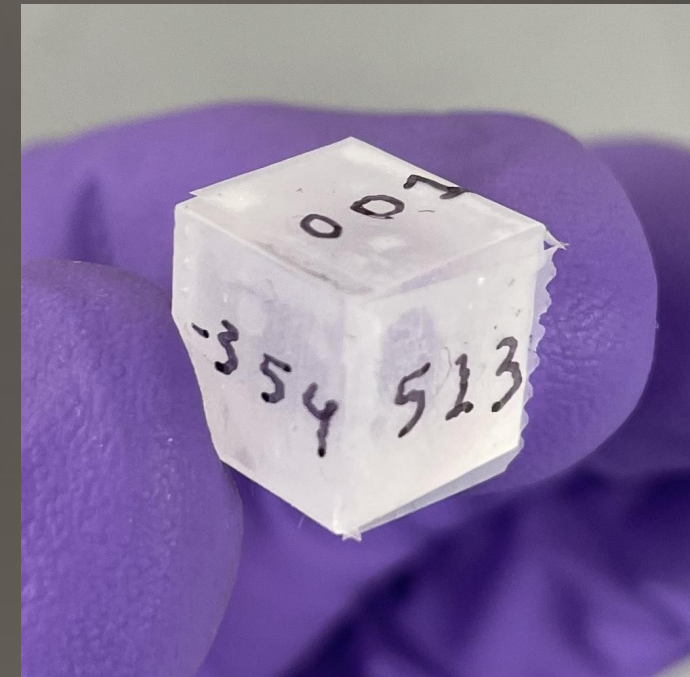
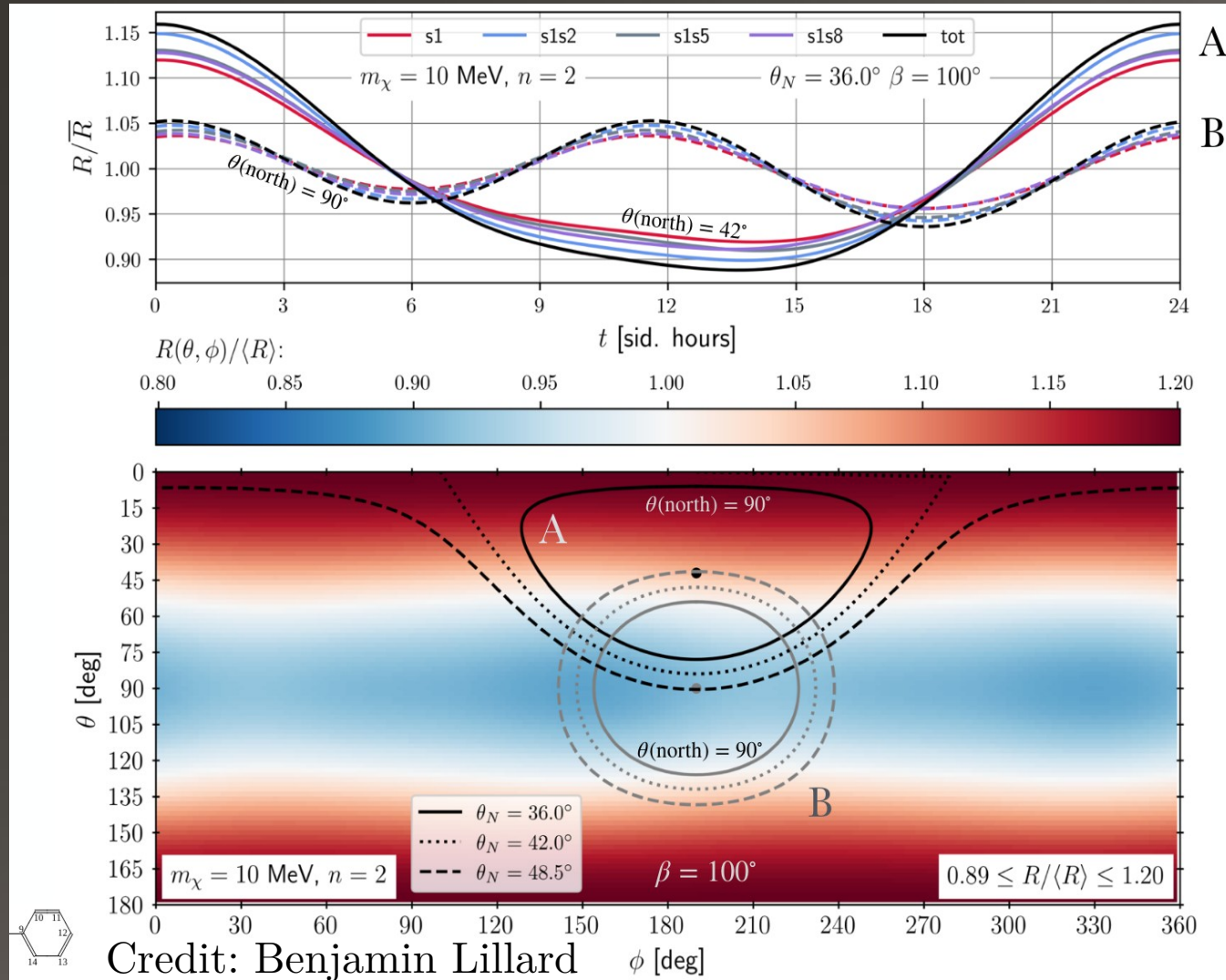
Molecular planes oriented in crystal lattice



Carman, et.al. '18 (J. of Crystal Growth)

Large optical-quality crystals

Looking for Daily Modulation



Different trajectories through rotation angles give distinct waveforms and phases. We can use the same crystal in many orientations or many different crystals.



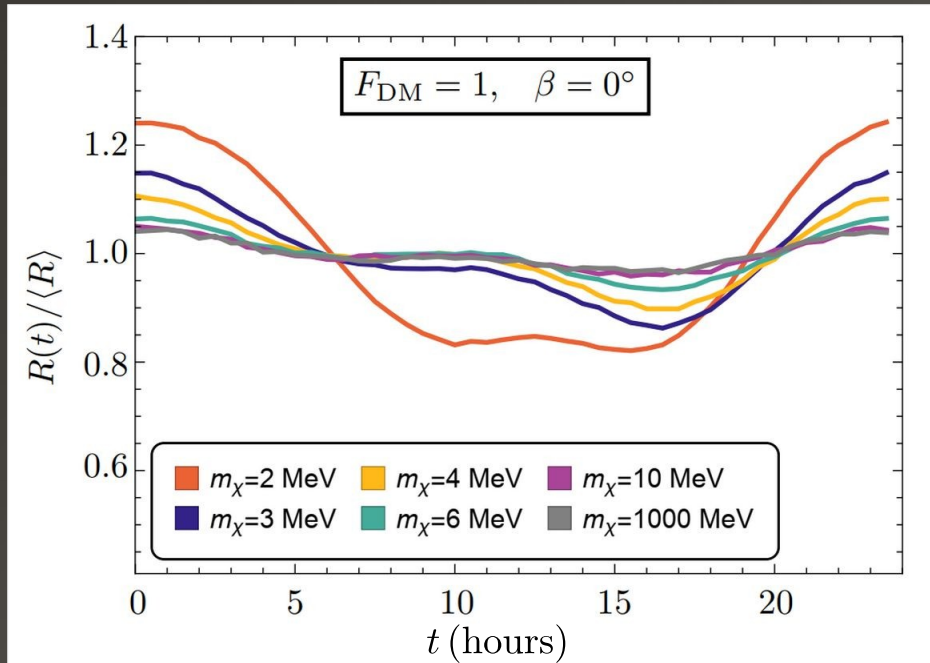
Credit: Benjamin Lillard ϕ [deg]

<https://github.com/blillard/vsdm>

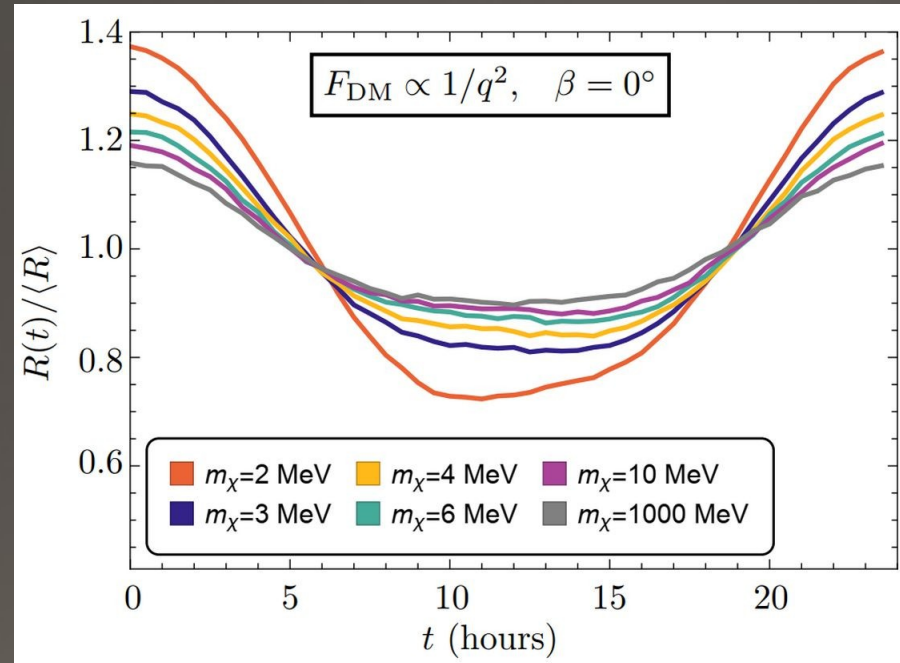
Carlos Blanco - 2025

Daily Modulation

(Contact interaction)



(Long-range interaction)



Predicted rate changes by up to 70% throughout the day.

That's a verifiable signal!

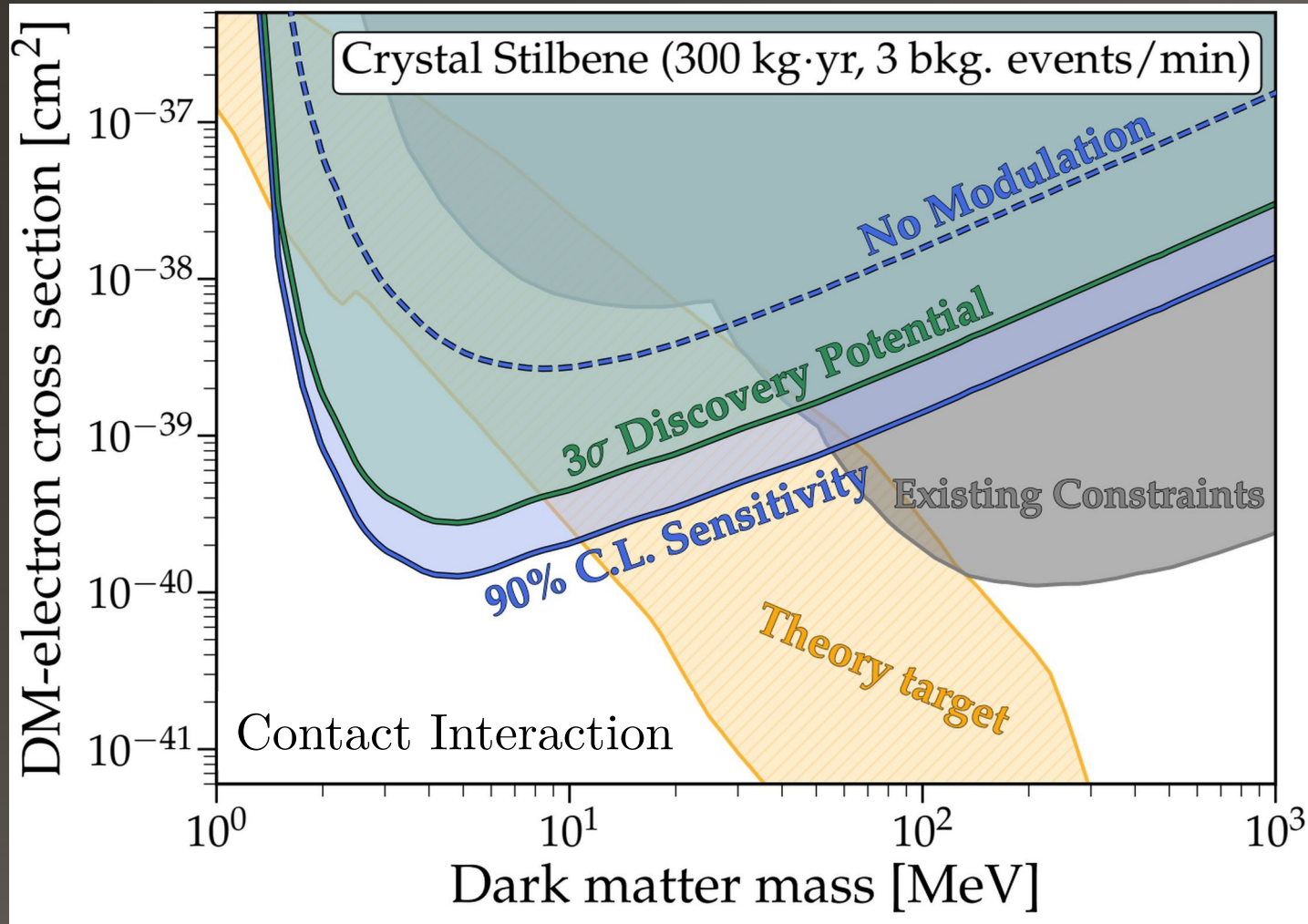
[CB, Kahn, Lillard, McDermott: 2103.08601]

Modulation amplitude remains as high as 10% even at the highest masses. This is due to the *fundamental anisotropy of the molecular form factor*.

$$f_{\text{RMS}} = [5\% - 25\%]$$

$$N_\sigma \sim f_{\text{RMS}} \sqrt{N_{\text{events}}}$$

Sensitivity & Reach



Assuming realistic backgrounds

Exclusion w/o modulation

Discovery potential w/ mod.

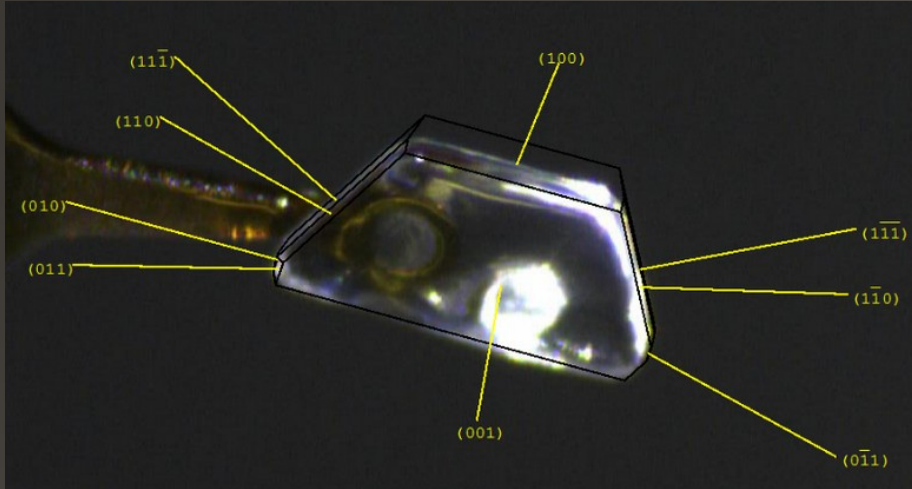
Exclusion w/ modulation

100 kg t-stilbene crystals exposed for 3 years w/ background rate of 3 events/min dominated by radioactivity of ^{14}C , Th, & U.

Consistent w/ Borexino $^{14}\text{C}/^{12}\text{C} \sim 10^{-18}$ (0.01/min/kg)

Characterizing t-stilbene

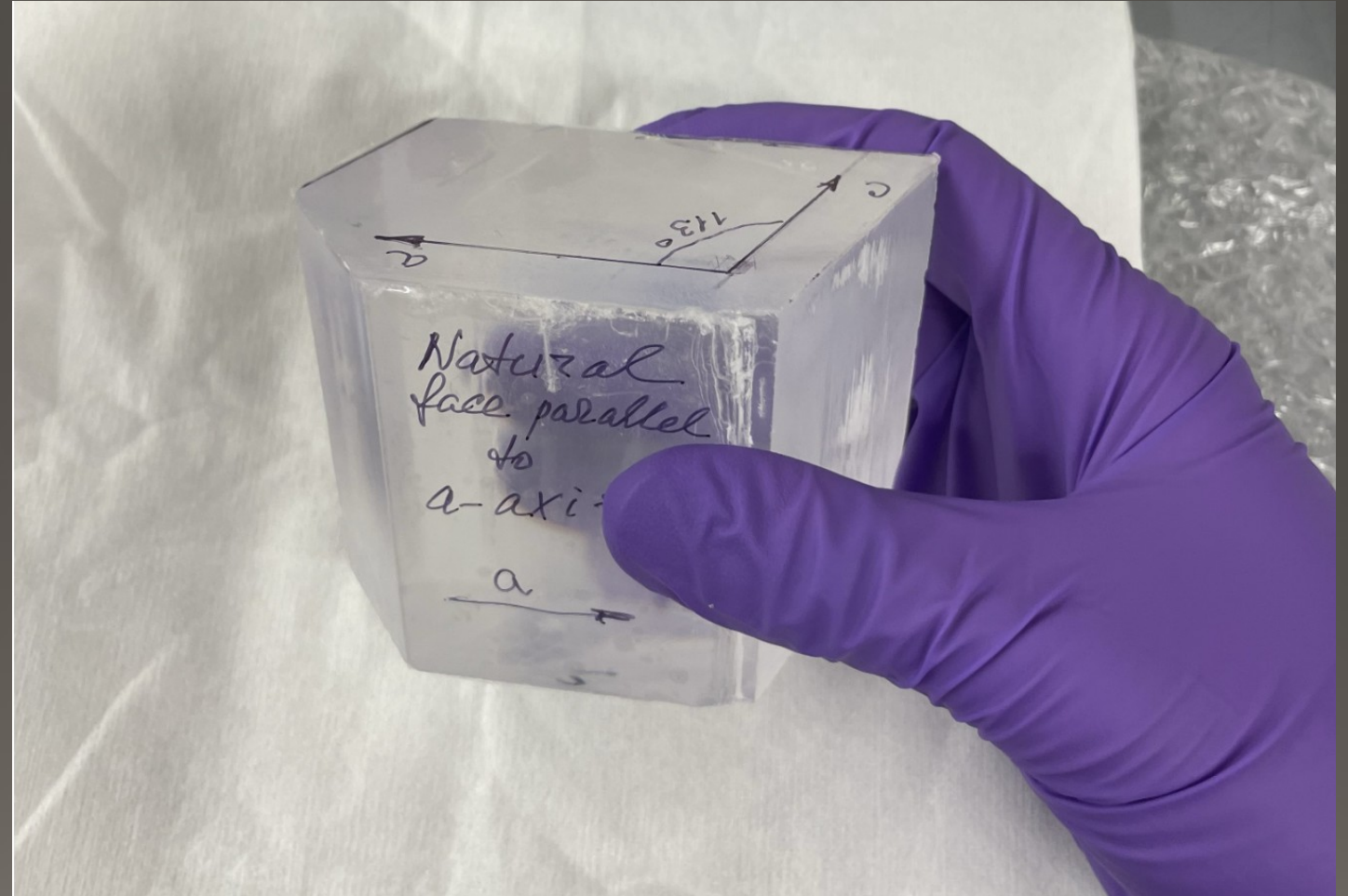
Calibrate at mg-scale



Credit: Dane Johnson
Freedman Group (MIT)

Natalia Zaitseva (LLNL)

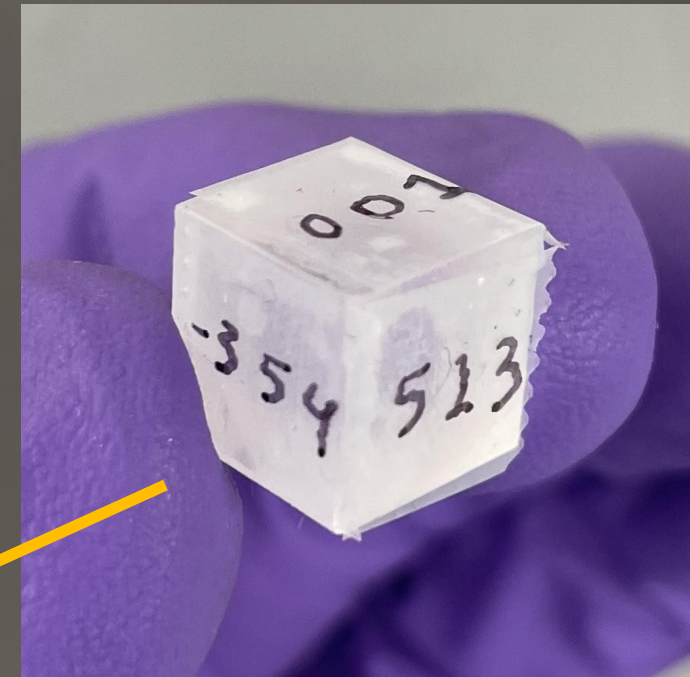
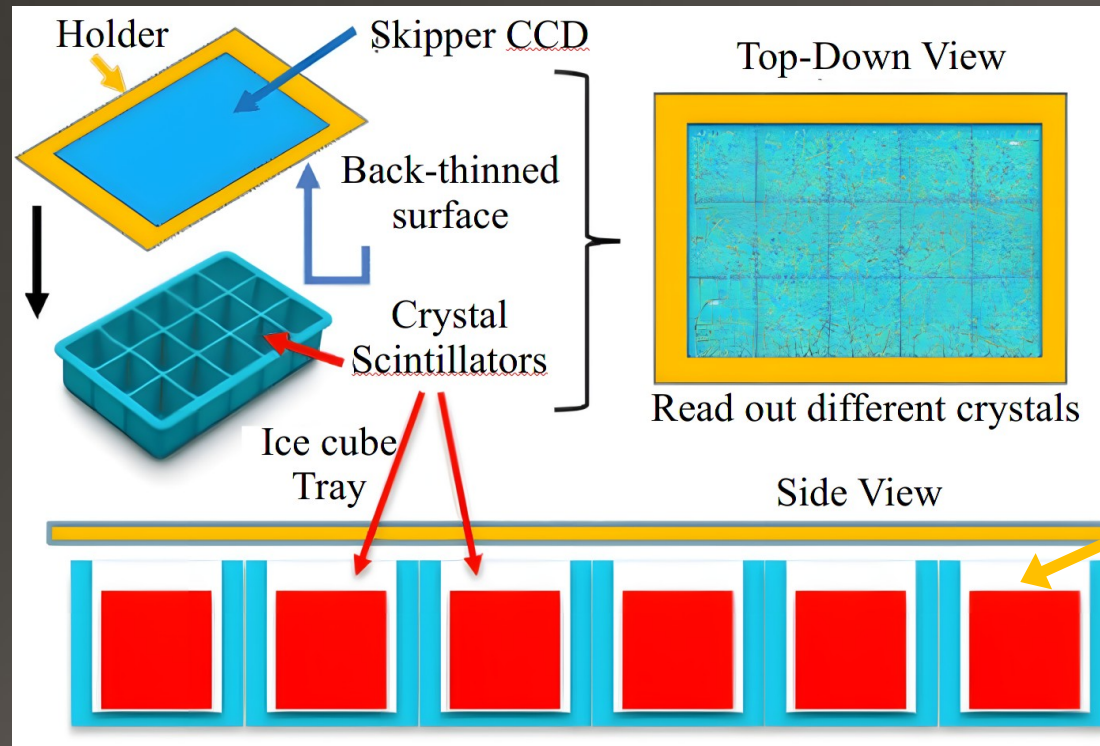
Deploy up to kg-scale



Experimental Deployment

DIANA*

Daily modulation in an Intrinsically ANisotropic Array



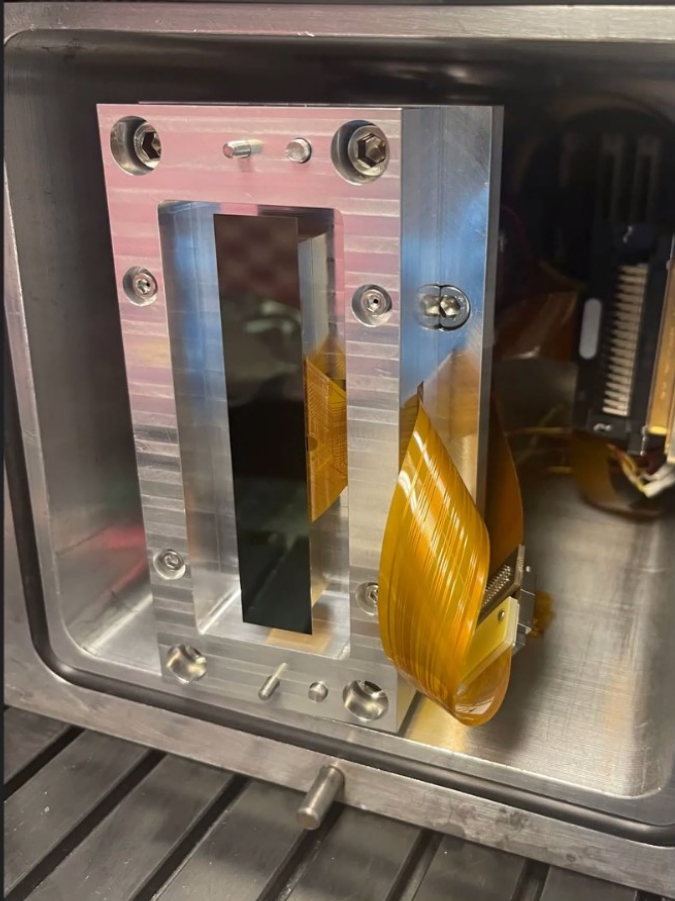
Many crystal samples can be read out by a single skipper CCD.

Collaboration: FermiLab, U. Toronto, MIT, UIUC, U. Oregon, Penn State

Astro-Skipper CCDs as Readout

Taking pictures of crystals with a *very* sensitive CCD

Skipper CCD Measurements of trans-Stilbene



Daniel Baxter, Alex Drlica-Wagner,
Edgar Marrufo, Brandon Roach

Calibrating Anisotropic Materials

Calibration of Anisotropy via Photoabsorption

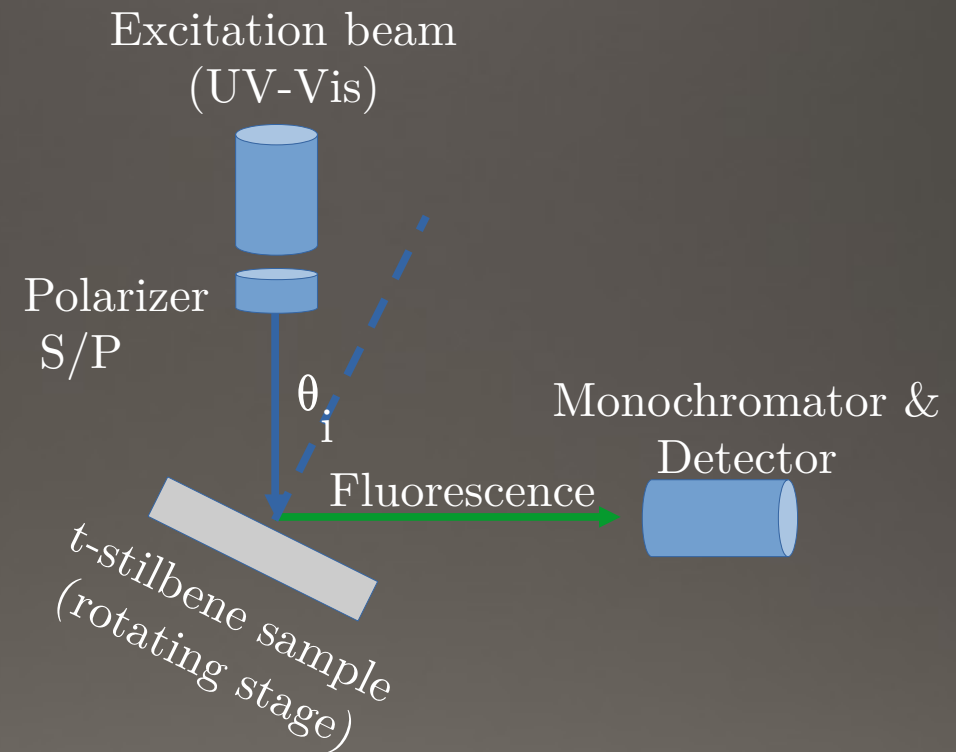
Dark Matter Scattering

$$\sigma_e \sim |f_{i \rightarrow f}(\mathbf{q})|^2 = |\langle \Psi_f | e^{i\mathbf{q} \cdot \mathbf{r}} | \Psi_i \rangle|^2$$
$$\approx |\mathbf{q} \cdot \langle \Psi_f | \mathbf{r} | \Psi_i \rangle|^2$$

UV photon absorption

$$\sigma_{\text{UV}} \sim (E_f - E_i) |\vec{\epsilon} \cdot \langle \Psi_f | \mathbf{r} | \Psi_i \rangle|^2$$

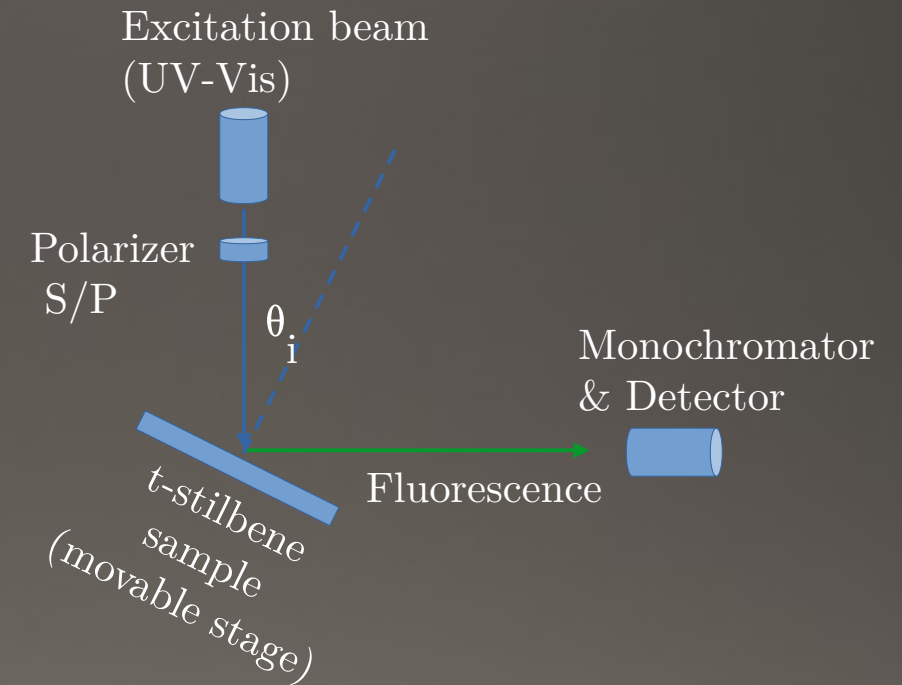
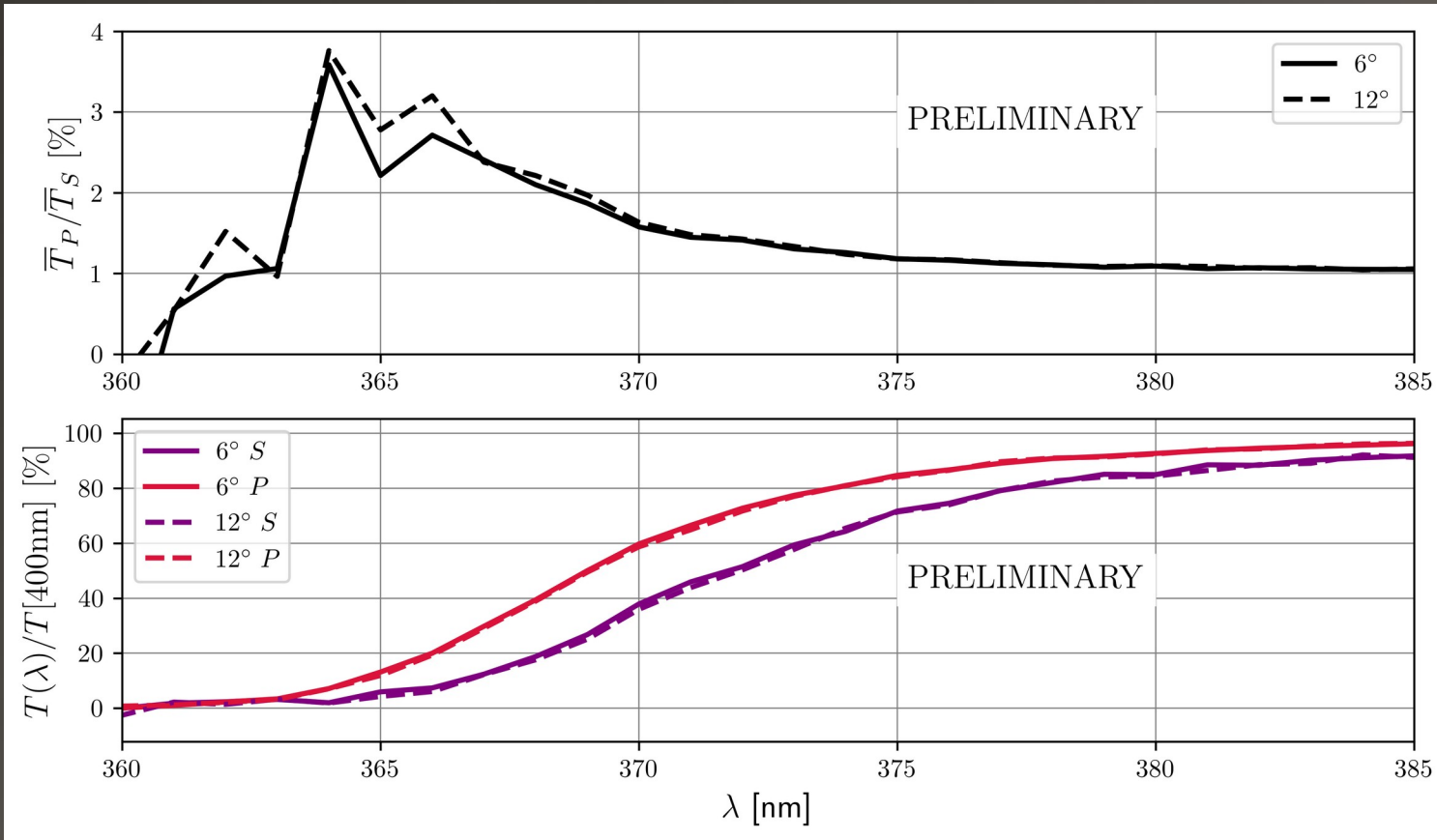
$$A_{\text{UV}} \sim n_{\text{mol}} |\vec{\epsilon} \cdot \langle \Psi_f | \mathbf{r} | \Psi_i \rangle|^2$$



Polarization is a proxy for DM momentum

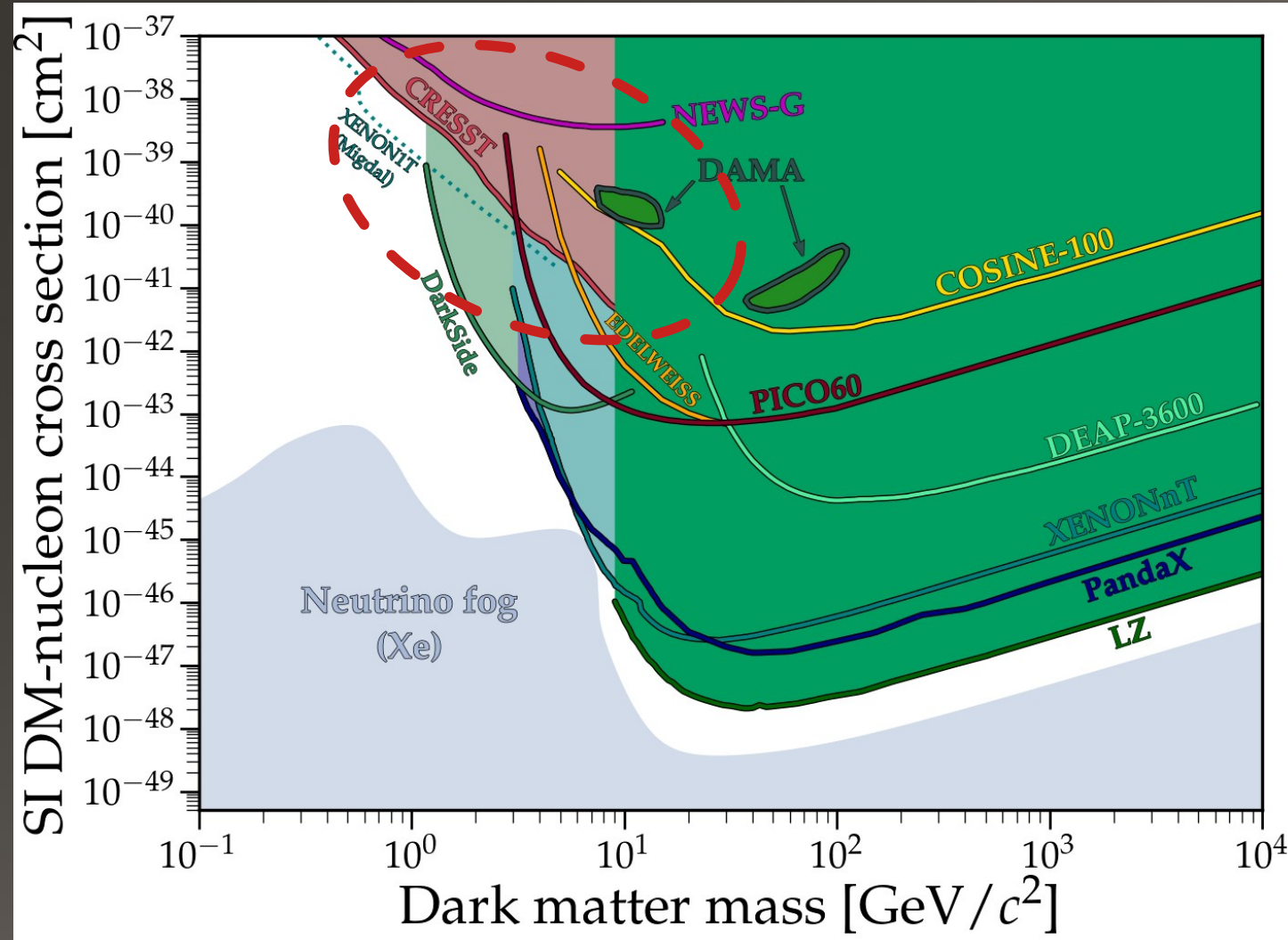
Calibrating Anisotropic Materials

Calibration of Anisotropy via Photoabsorption



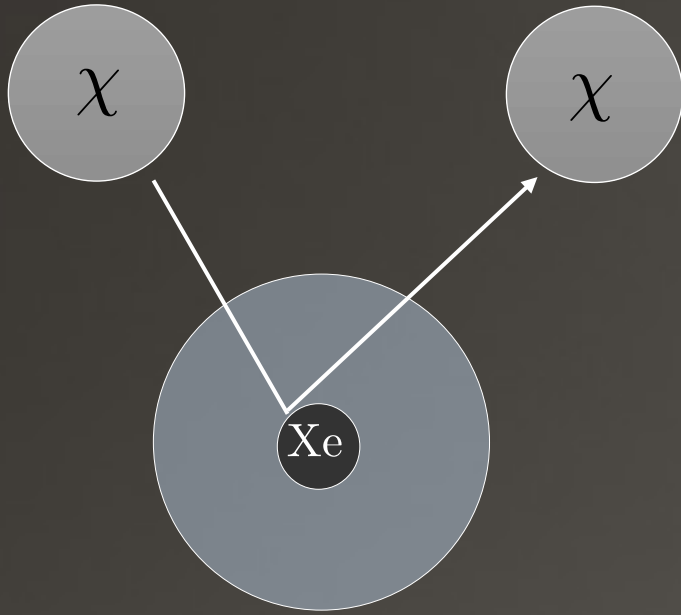
$$A_{UV} \sim n_{\text{mol}} |\vec{\epsilon} \cdot \langle \Psi_f | \mathbf{r} | \Psi_i \rangle|^2 \quad A_{UV} \approx \text{const} - T_{UV}$$

Migdal in Liquid Noble Gas TPCs



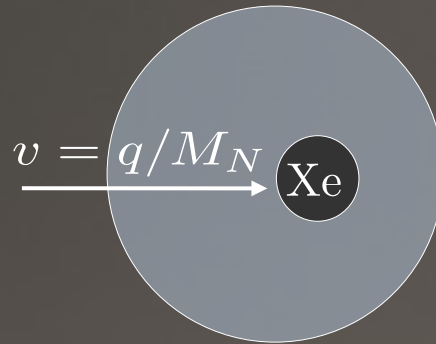
Migdal effect extends sensitivity from few GeV to 100s MeV

Ionizing Atoms Through Nuclear Recoil: Migdal Effect

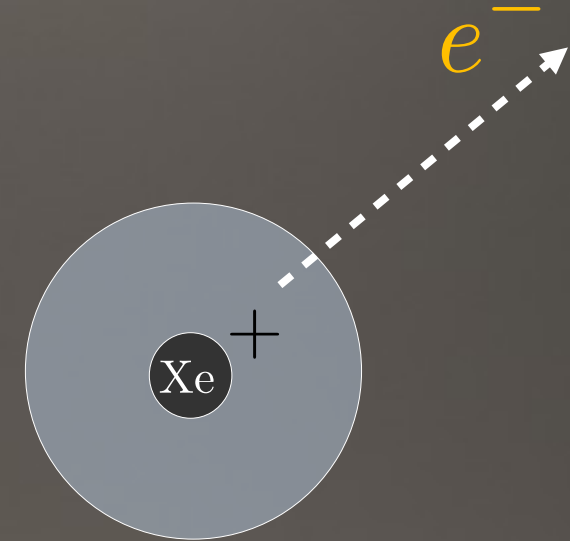


Initial nuclear recoil

$$|\psi_i\rangle \sim e^{i \frac{m_e}{M_N} \vec{q} \cdot \vec{r}} \psi_{\text{AO}}(r_\beta)$$



Nucleus moves faster than electrons



Electronic transition to ionized state

The Migdal effect

Inelasticity extends the sensitivity of detectors to lower masses. e.g. Xenon

$$f_{i \rightarrow f} \approx \frac{m_e}{M_N} \vec{q} \cdot \langle \vec{r} \rangle_{i \rightarrow f}$$

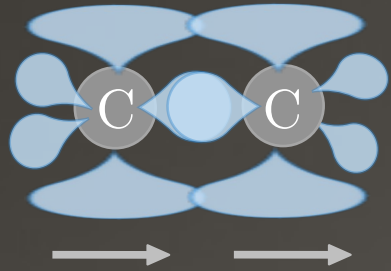
Kinematic *penalty*

The Molecular Migdal Effect(s)

Sensitivity to Nuclear Recoils

Center of mass recoil (CMR) effect

Caused by center of mass motion



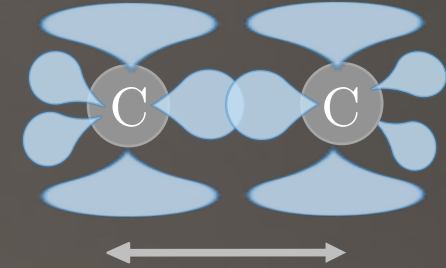
COM recoil effect is the molecular analog of the semiclassical Migdal effect

$$P_{CMR} \sim \frac{m_e}{M_{mol}}$$

Suppressed by kinematic factor due to moving the whole molecule.

Non-adiabatic coupling (NAC) effect

Caused by relative motion



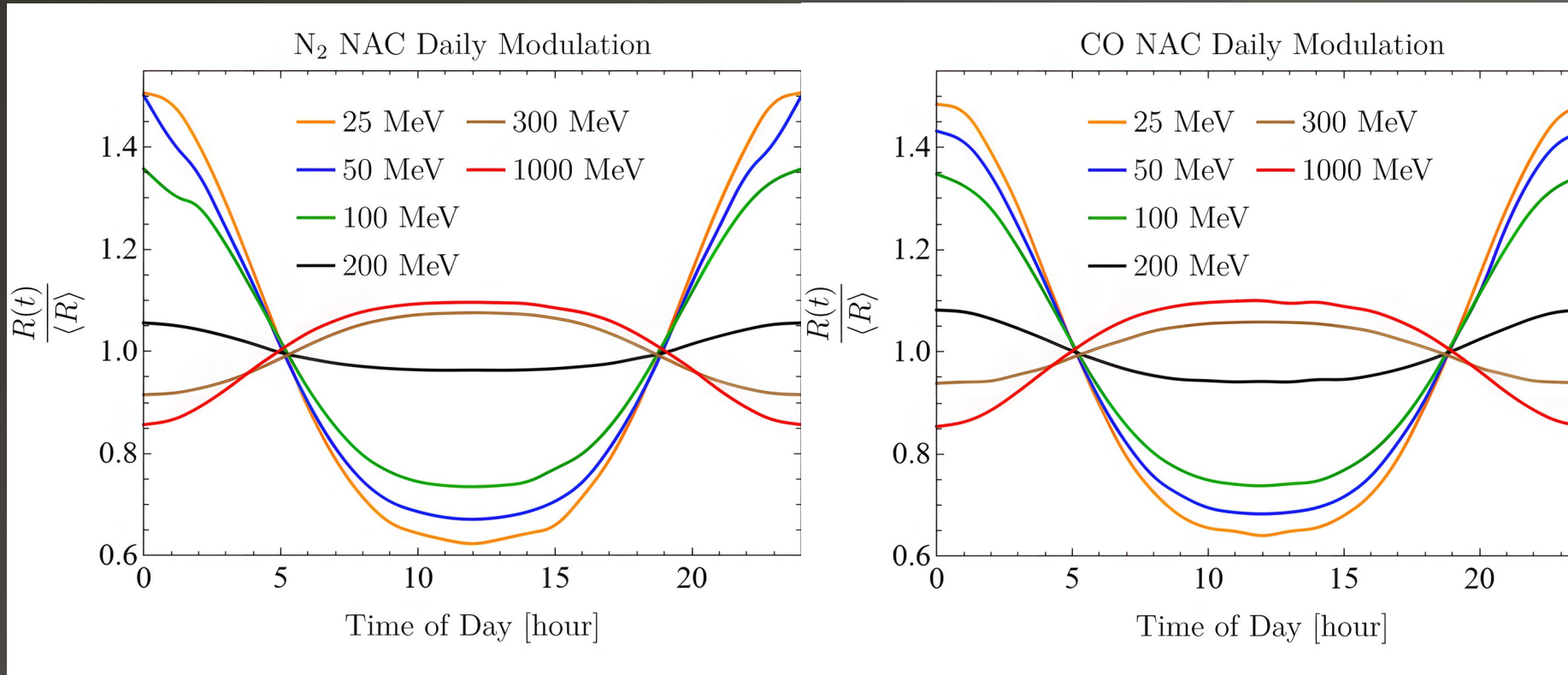
NAC caused by effects beyond Born-Oppenheimer approximation

$$P_{NAC} \sim \frac{m_e}{M_N}$$

Suppressed by kinematic factor due to moving a single atom.

Directional Molecular Migdal Effect

[CB, Harris*, Kahn, Lillard, Perez-Rios: 2208.09002]



Predicted rate changes by up to 80% throughout the day.

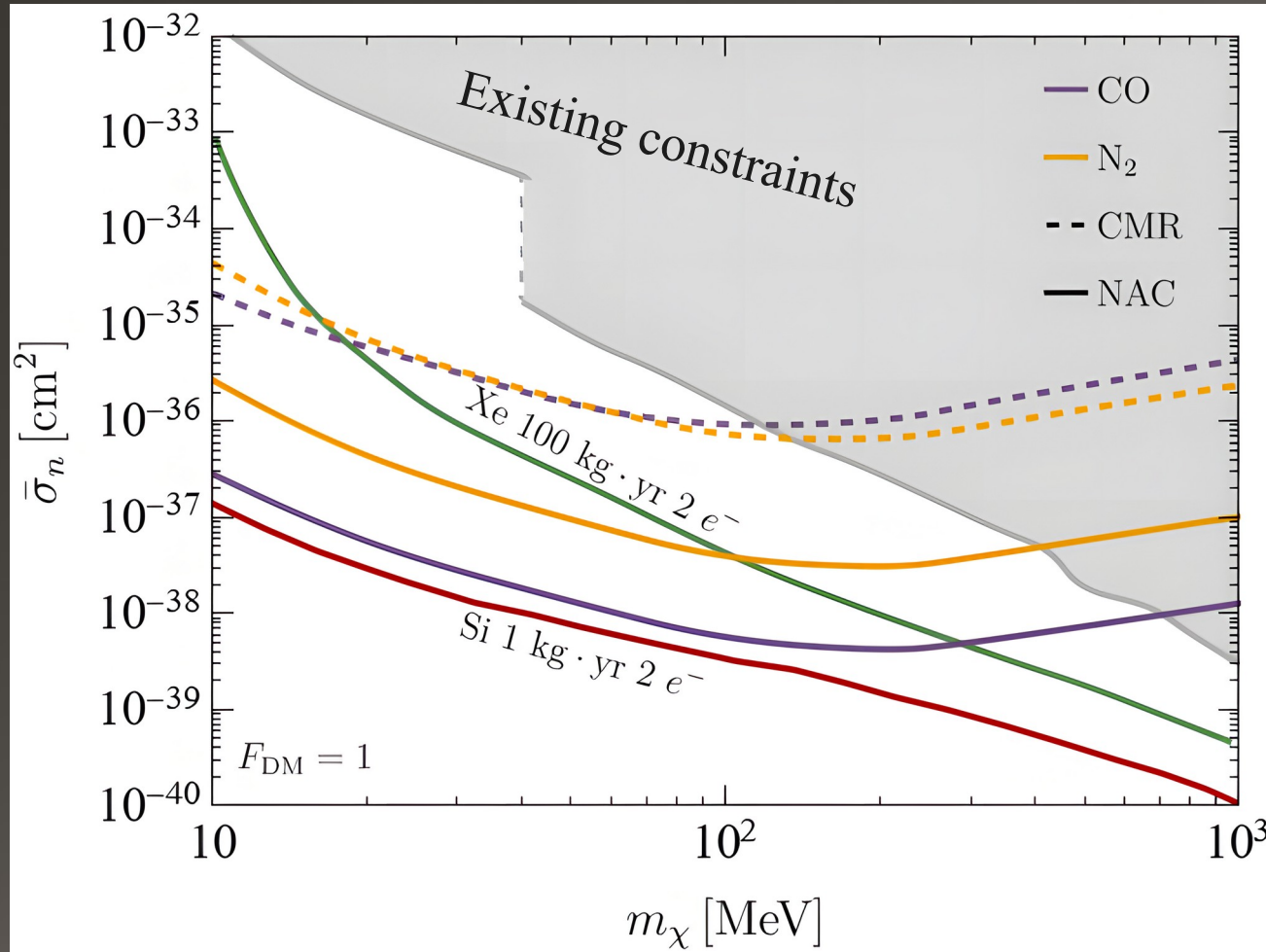
The daily modulation phase is mass dependent.

Persistent daily modulation at large dark matter mass is generically predicted for the molecular Migdal effects. We predict that the same class of molecules that make good directional detectors for electron scattering will also be ideal for nuclear scattering because of the directional molecular Migdal effects.

The Molecular Migdal Effect(s)

Sensitivity to Nuclear Recoils

(Contact interaction)



Si rate is entirely due to non-adiabatic processes. [Esposito & Rocchi 2505.08864]

← *Center of mass recoil* effect is predicted to be subdominant at all masses.

← *Non-adiabatic coupling* effect is predicted to dominate due to favorable kinematic factor.

Simplest molecular models already competitive.

Is there an optimal molecular target?

Anisotropic Materials

2D Targets: e.g. graphene, MoS₂, GaN

Polar Semiconductors: e.g. Al₂O₃, SiC, GaAs, Eu₅In₂Sb₆ (SPLENDOR)

Dirac materials: e.g. ZrTe₅

Crystalline scintillators:

e.g. NaI, GaAs, trans-stilbene, etc...

Need

- > 10 kg low-background material
- Large anisotropy, $N_\sigma \sim f_{RMS} (m T_{exp})^{1/2}$

Y. Hochberg, Y. Kahn, M. Lisanti, C. G. Tully and K. M. Zurek, *Directional detection of dark matter with two-dimensional targets*, Phys. Lett. B **772**, 239 (2017), doi:[10.1016/j.physletb.2017.06.051](https://doi.org/10.1016/j.physletb.2017.06.051), [1606.08849](https://arxiv.org/abs/1606.08849).

R. Budnik, O. Chesnovsky, O. Slone and T. Volansky, *Direct Detection of Light Dark Matter and Solar Neutrinos via Color Center Production in Crystals*, Phys. Lett. B **782**, 242 (2018), doi:[10.1016/j.physletb.2018.04.063](https://doi.org/10.1016/j.physletb.2018.04.063), [1705.03016](https://arxiv.org/abs/1705.03016).

Y. Hochberg, Y. Kahn, M. Lisanti, K. M. Zurek, A. G. Grushin, R. Ilan, S. M. Griffin, Z.-F. Liu, S. F. Weber and J. B. Neaton, *Detection of sub-MeV Dark Matter with Three-Dimensional Dirac Materials*, Phys. Rev. D **97**(1), 015004 (2018), doi:[10.1103/PhysRevD.97.015004](https://doi.org/10.1103/PhysRevD.97.015004), [1708.08929](https://arxiv.org/abs/1708.08929).

S. Griffin, S. Knapen, T. Lin and K. M. Zurek, *Directional Detection of Light Dark Matter with Polar Materials*, Phys. Rev. D **98**(11), 115034 (2018), doi:[10.1103/PhysRevD.98.115034](https://doi.org/10.1103/PhysRevD.98.115034), [1807.10291](https://arxiv.org/abs/1807.10291).

A. Coskuner, A. Mitridate, A. Olivares and K. M. Zurek, *Directional Dark Matter Detection in Anisotropic Dirac Materials*, Phys. Rev. D **103**(1), 016006 (2021), doi:[10.1103/PhysRevD.103.016006](https://doi.org/10.1103/PhysRevD.103.016006), [1909.09170](https://arxiv.org/abs/1909.09170).

R. M. Geilhufe, F. Kahlhoefer and M. W. Winkler, *Dirac Materials for Sub-MeV Dark Matter Detection: New Targets and Improved Formalism*, Phys. Rev. D **101**(5), 055005 (2020), doi:[10.1103/PhysRevD.101.055005](https://doi.org/10.1103/PhysRevD.101.055005), [1910.02091](https://arxiv.org/abs/1910.02091).

S. M. Griffin, Y. Hochberg, K. Inzani, N. Kurinsky, T. Lin and T. Chin, *Silicon carbide detectors for sub-GeV dark matter*, Phys. Rev. D **103**(7), 075002 (2021), doi:[10.1103/PhysRevD.103.075002](https://doi.org/10.1103/PhysRevD.103.075002), [2008.08560](https://arxiv.org/abs/2008.08560).

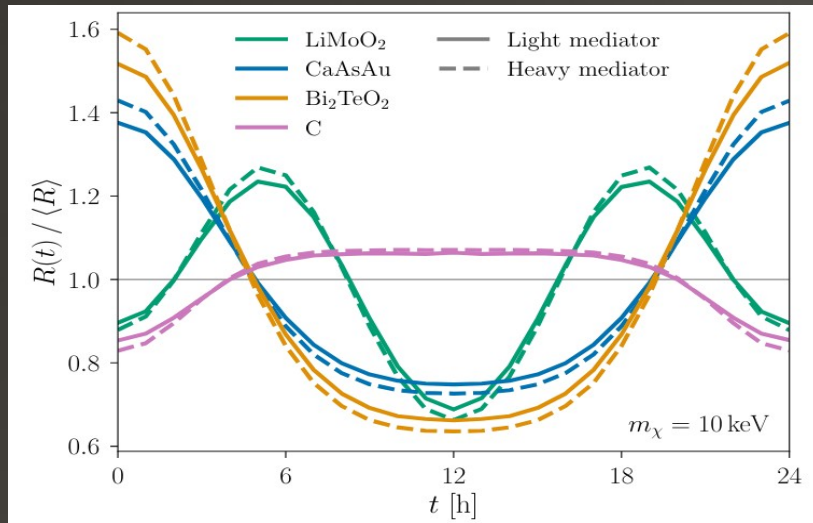
C. Blanco, Y. Kahn, B. Lillard and S. D. McDermott, *Dark Matter Daily Modulation With Anisotropic Organic Crystals*, Phys. Rev. D **104**, 036011 (2021), doi:[10.1103/PhysRevD.104.036011](https://doi.org/10.1103/PhysRevD.104.036011), [2103.08601](https://arxiv.org/abs/2103.08601).

A. Coskuner, T. Trickle, Z. Zhang and K. M. Zurek, *Directional detectability of dark matter with single phonon excitations: Target comparison*, Phys. Rev. D **105**(1), 015010 (2022), doi:[10.1103/PhysRevD.105.015010](https://doi.org/10.1103/PhysRevD.105.015010), [2102.09567](https://arxiv.org/abs/2102.09567).

C. Blanco, I. Harris, Y. Kahn, B. Lillard and J. Pérez-Ríos, *Molecular Migdal effect*, Phys. Rev. D **106**(11), 115015 (2022), doi:[10.1103/PhysRevD.106.115015](https://doi.org/10.1103/PhysRevD.106.115015), [2208.09002](https://arxiv.org/abs/2208.09002).

C. Boyd, Y. Hochberg, Y. Kahn, E. D. Kramer, N. Kurinsky, B. V. Lehmann and T. C. Yu, *Directional detection of dark matter with anisotropic response functions* (2022), [2212.04505](https://arxiv.org/abs/2212.04505).

Mining for Crystals in Data



First High-throughput evaluation of Dark Matter Detector Materials

- Used the crystals in the Material Project
- Fit anisotropic Lindhard dielectric tensor to data

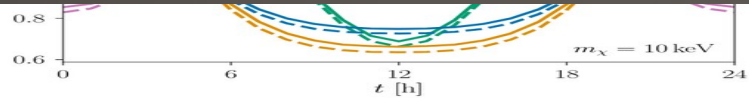
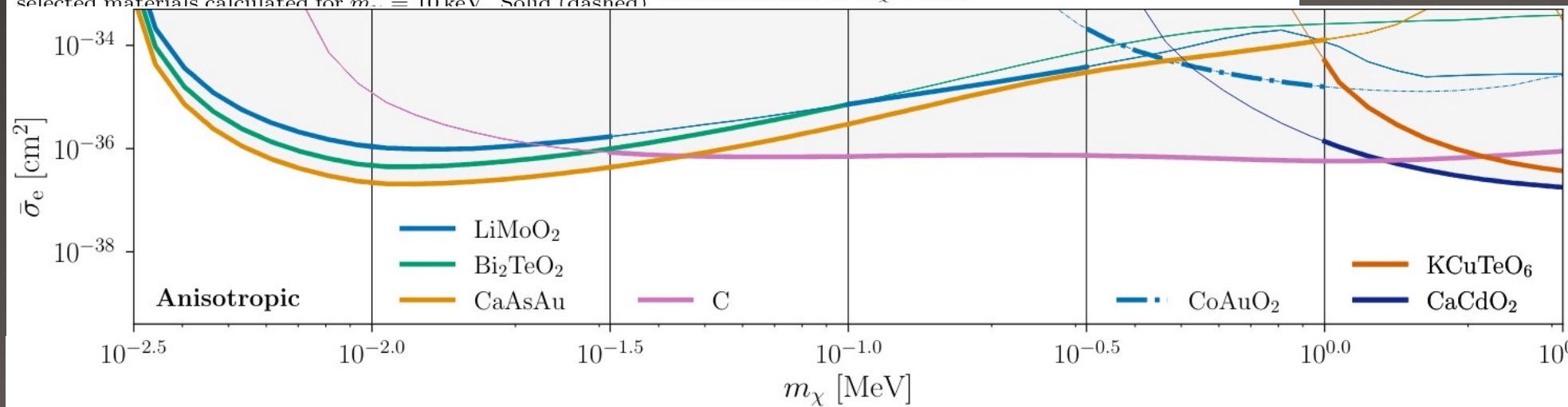


FIG. 3. Daily modulation of the DM scattering rate for four selected materials calculated for $m_\chi = 10$ keV. Solid (dashed) lines correspond to a light (heavy) mediator. The materials CaCdO₂, CoAuO₂, and KCuTeO₆ exhibit daily modulations of similar order at $m_\chi \sim$ MeV.



Inventing Optimal Targets

Problem: Chemical space is unreasonably large

How many molecules possible with
C, O, N, F, H?

< 9 atoms: 100s of Thousands (DFT Computable)

< 30 atoms: 100s of Billions (Intractable)

...toluene has 15, xylene has 18, t-stilbene has 26

Method

1. Look for known favorable properties - *cheminformatics*
2. Extra(intra)polate onto new molecules – *machine learning*

ML for DM Direct Detection

Property prediction Molecular Generation

Energies & Matrix elements Sample latent space \rightarrow new molecules

Small molecules : Using exhaustive database (< 9 atoms)

Characterize neural nets

\rightarrow Prove it's possible to learn from small subsample

Large molecules: Sparse dataset up to 10s of atoms

Scale architecture

\rightarrow Generate candidate molecule *shortlist*

Dataset of energies + oscillator strengths:

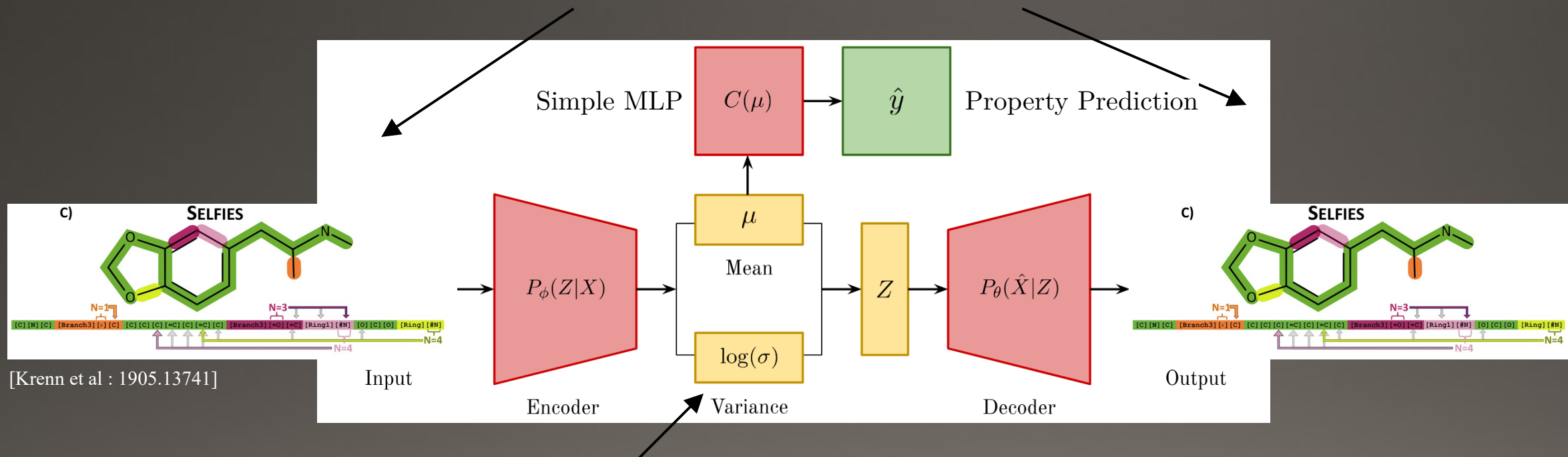
PubChemQ: a dataset of ~ 3 M organic molecules *computed* using Density Functional Theory

ML for DM Direct Detection

Molecular Space: Variational Autoencoders

Energies & Matrix elements Sample latent space \rightarrow new molecules

Discrete and sparse data space



Continuous latent space

Regression Model in Action

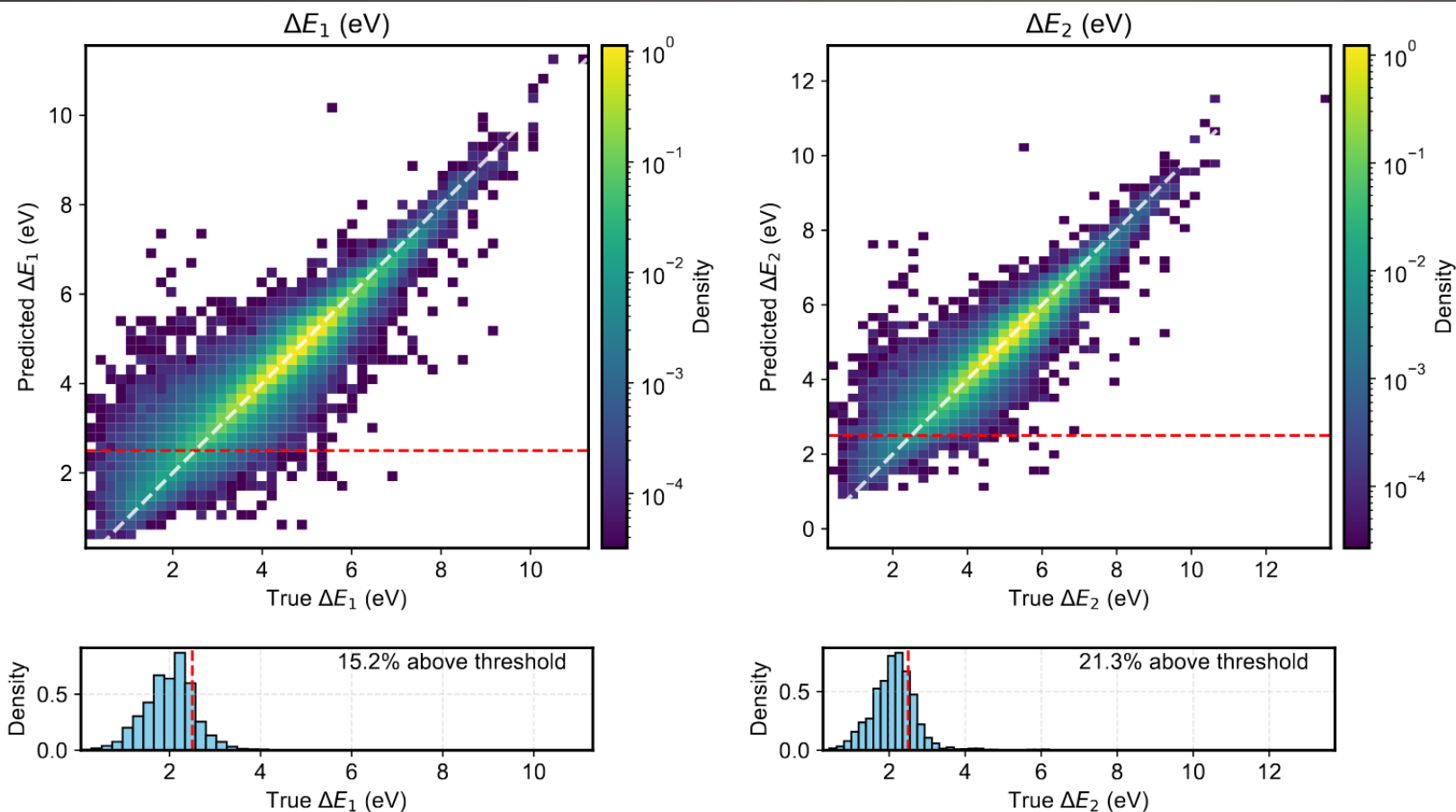


FIG. 19. We show the density of predicted values vs true values for the transition energies of our validation set, with a red line that corresponds to the threshold placed on the predicted value. The Histogram shows the distribution of true values for molecules whose predicted value is above the threshold.

Regression Model in Action

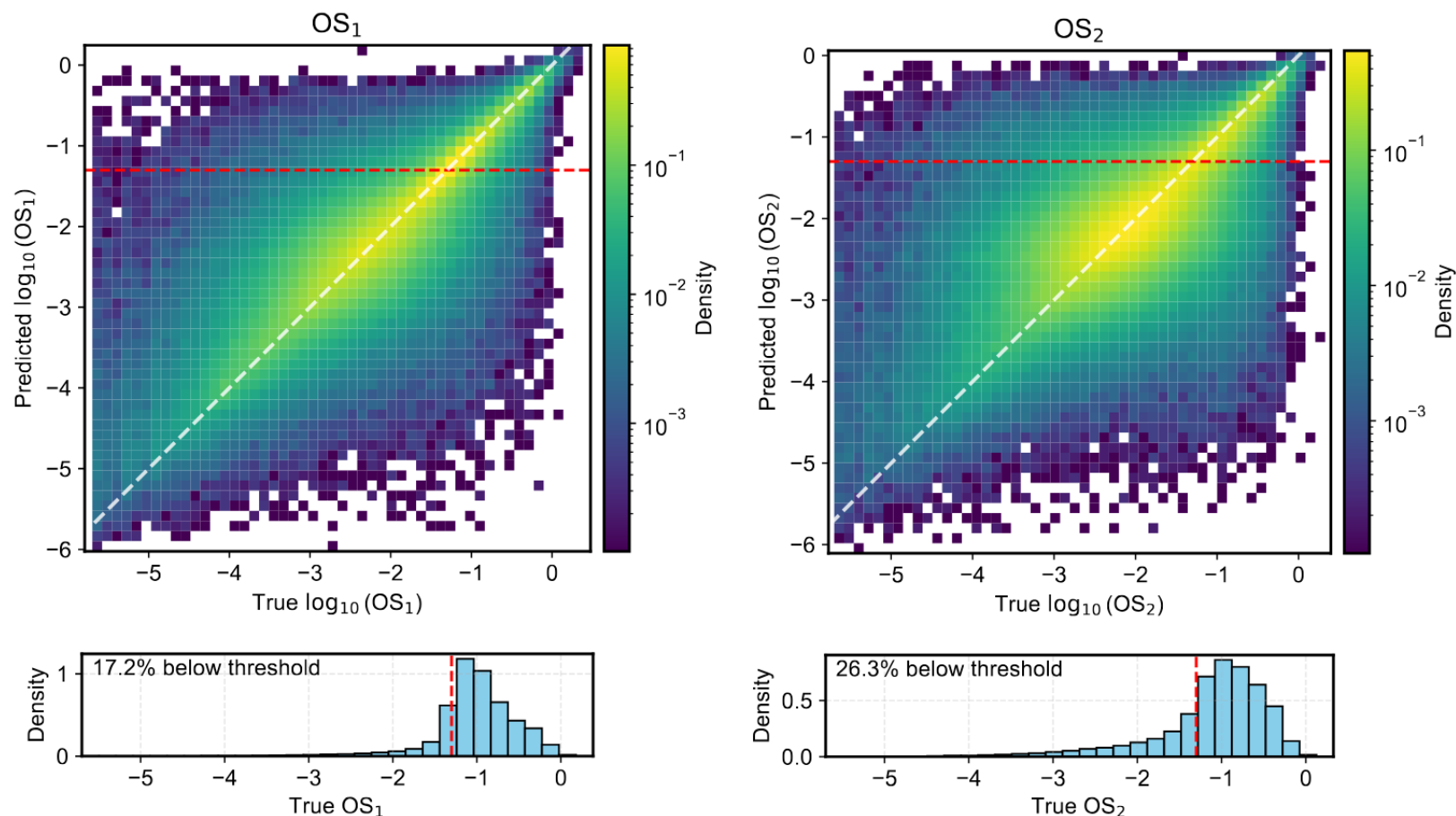


FIG. 20. We show the density of predicted values vs true values for the oscillator strength of our validation set, with a red line that corresponds to the threshold placed on the predicted value. The Histogram shows the distribution of true values for molecules whose predicted value is above the threshold.

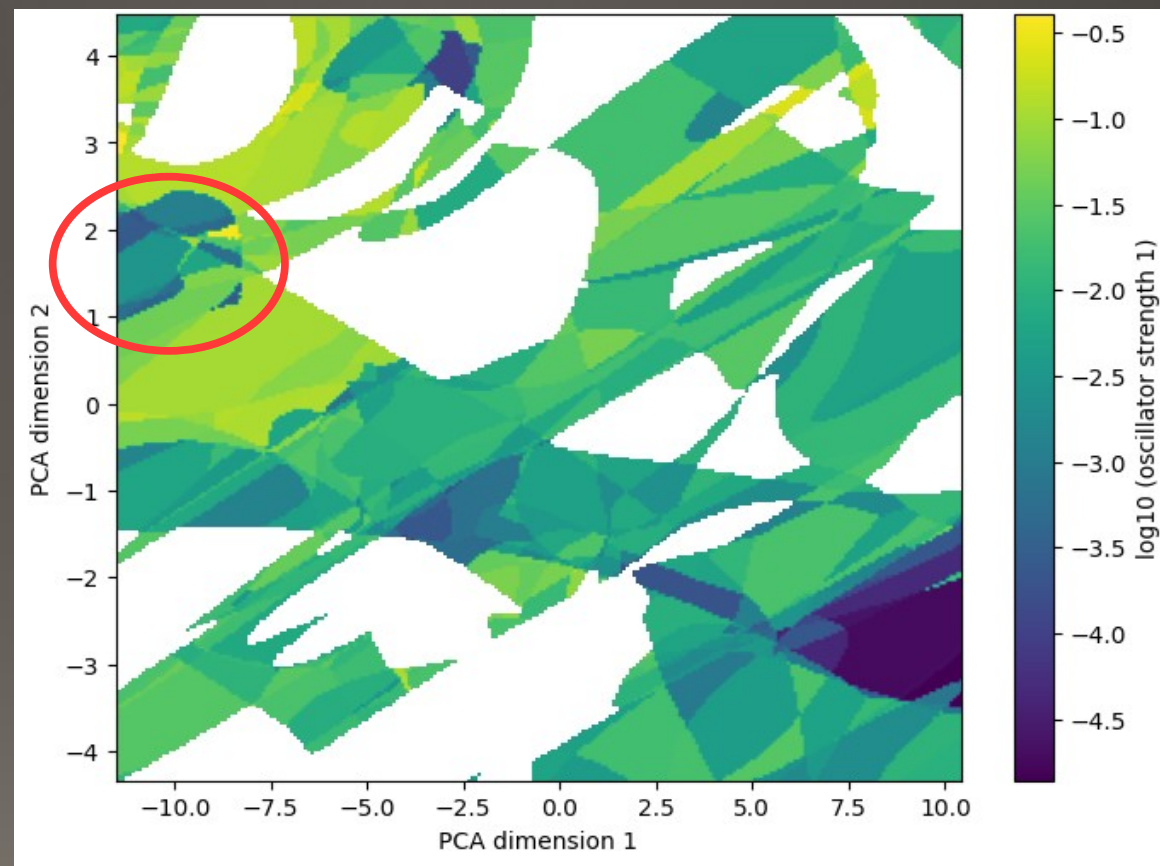
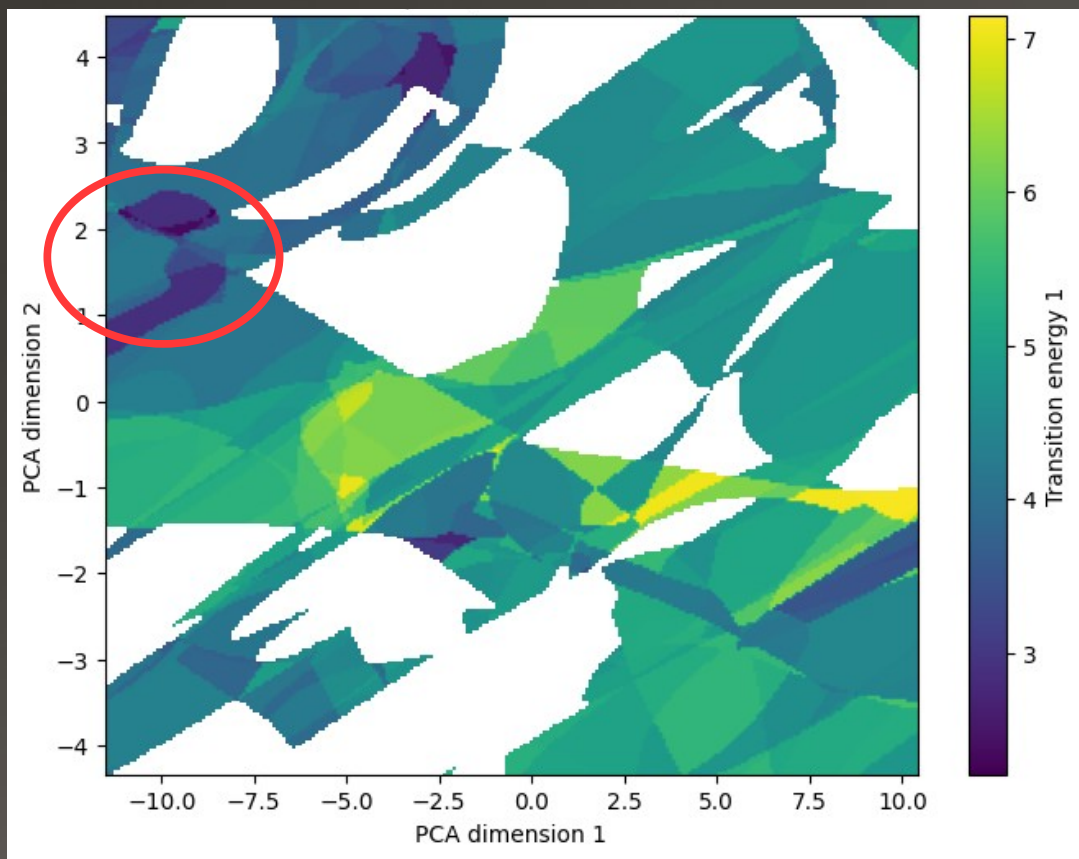
ML for DM Direct Detection

Property prediction: Molecular latent space

Energies & Matrix elements Sample latent space \rightarrow new molecules

$$\Delta E$$

$$\langle r_{01} \rangle \approx |f_{0,1}|/q$$



Clustering: Results

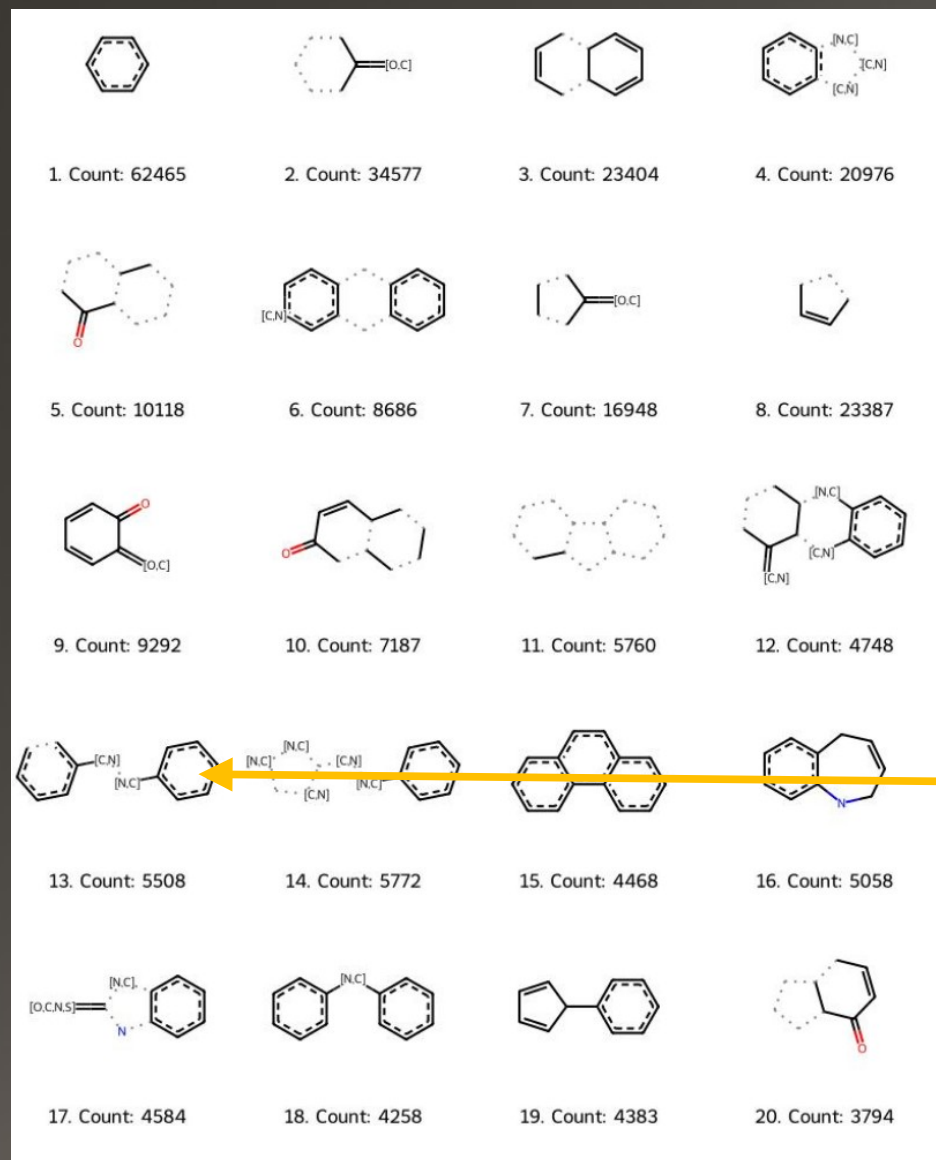
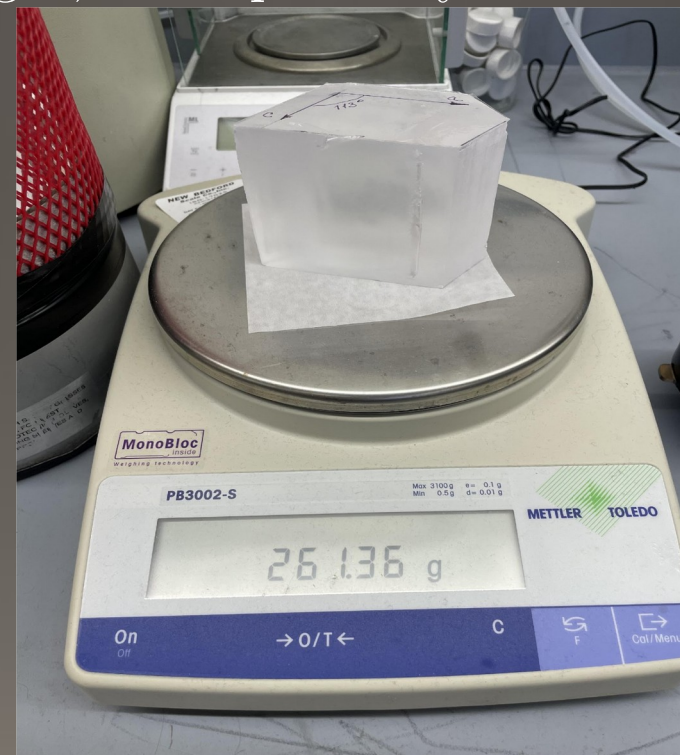



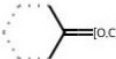
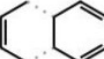
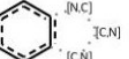
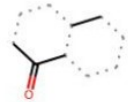

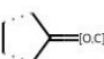

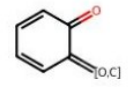
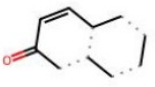

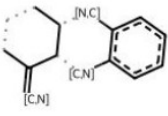
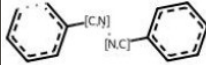
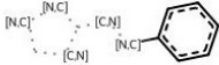

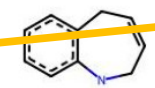
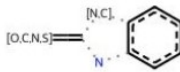
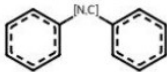
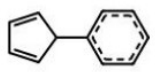
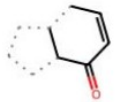
FIG. 7. Top 20 molecular motifs ranked by score. Note that certain atoms can be substituted by [C,N,O,S] as long as the structure remains isoelectronic. Dotted lines indicate that the bond could be a double or single bond.

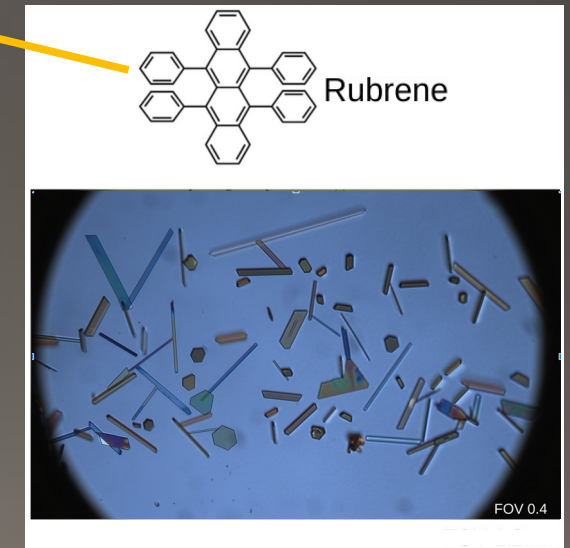
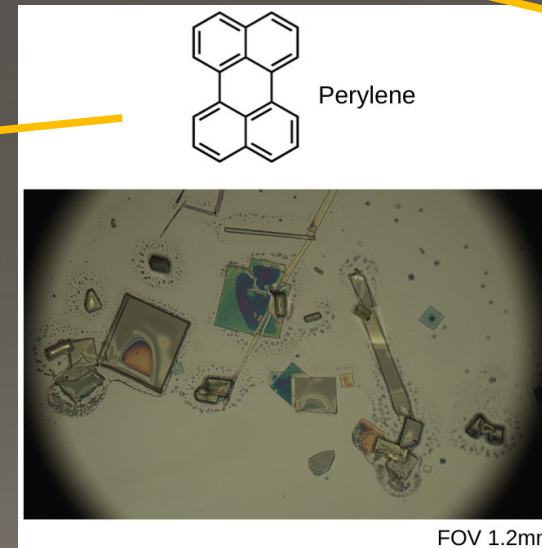
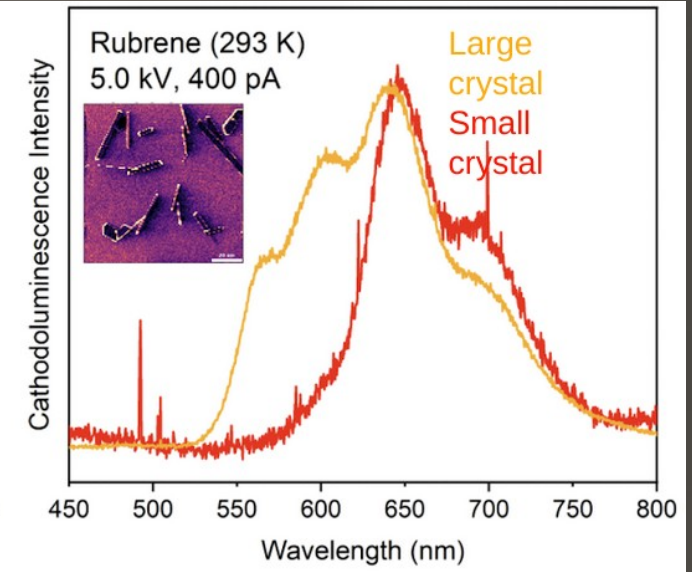
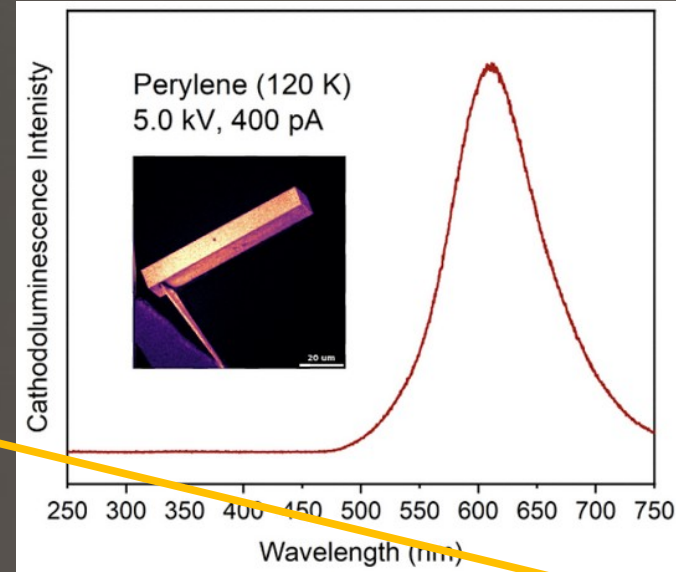
[C. Cook*, CB, J. Smirnov 2501.00091]

In hindsight, we're probably on the right track.



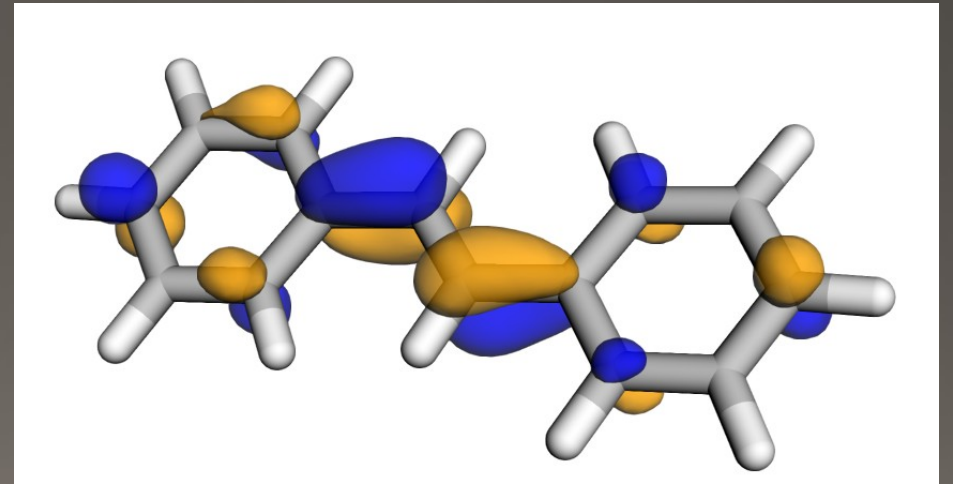
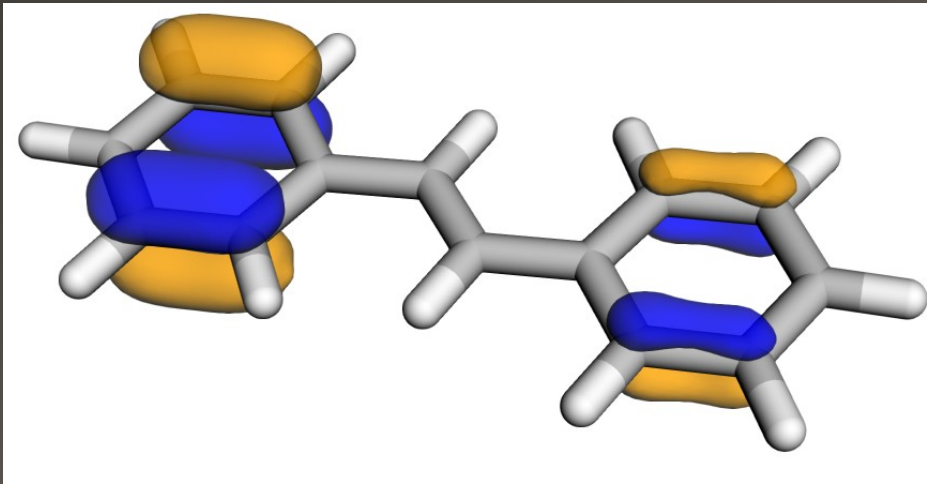
New Target Materials

			
1. Count: 62465	2. Count: 34577	3. Count: 23404	4. Count: 20976
			
5. Count: 10118	6. Count: 8686	7. Count: 16948	8. Count: 23387
			
9. Count: 9292	10. Count: 7187	11. Count: 5760	12. Count: 4748
			
13. Count: 5508	14. Count: 5772	15. Count: 4468	16. Count: 5058
			
17. Count: 4584	18. Count: 4258	19. Count: 4383	20. Count: 3794

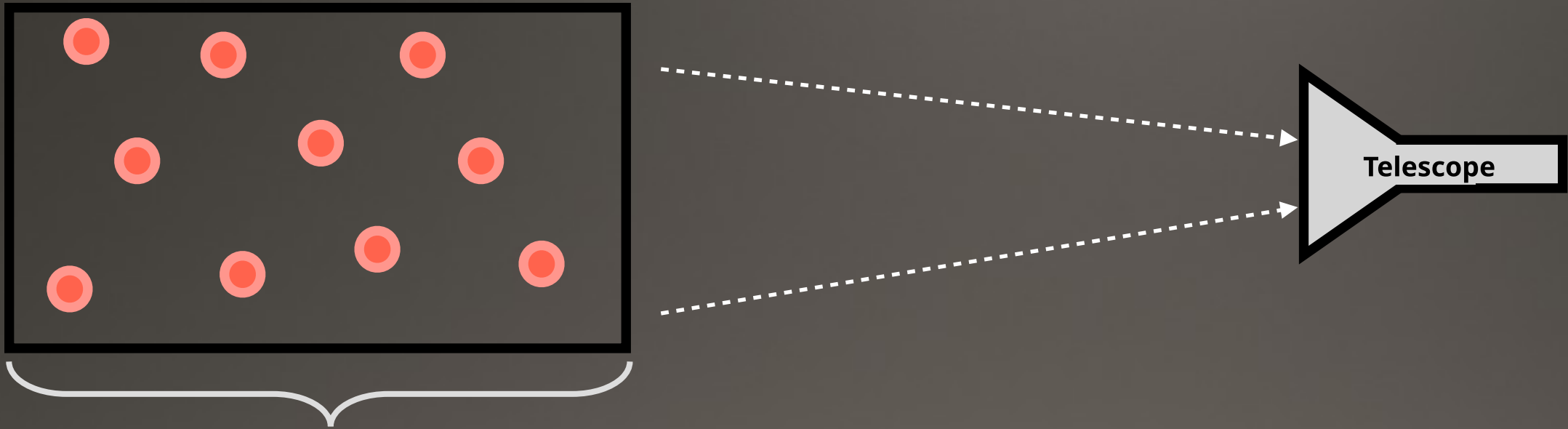


Conclusions

- 1) We have done an extremely effective job looking for WIMPs above a GeV, now we must look beyond.
- 2) By developing the formalism that describes the interaction between dark matter and molecules, we can develop detection strategies capable of *delving deep* and *searching wide* across the dark matter parameter space.



Beyond direct detection



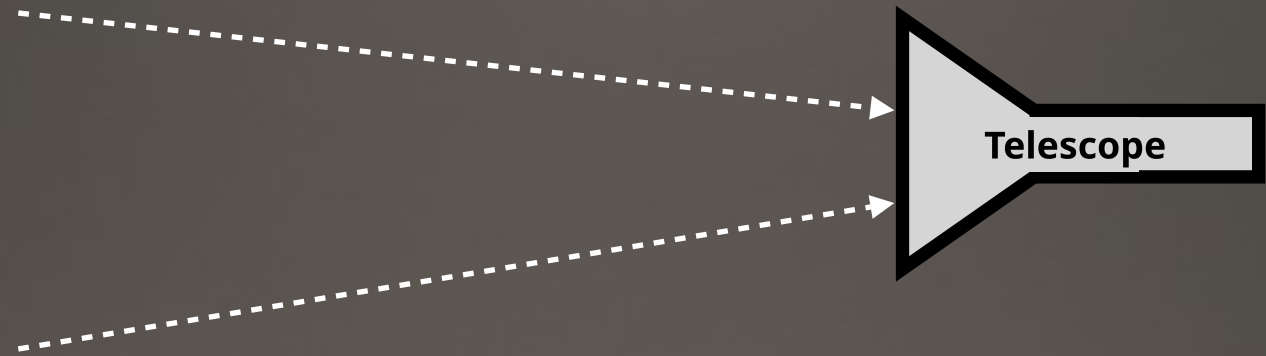
Astrophysical volume of molecules

We can use the same theoretical techniques that we've developed to predict rates in *astrophysical* objects

Beyond direct detection

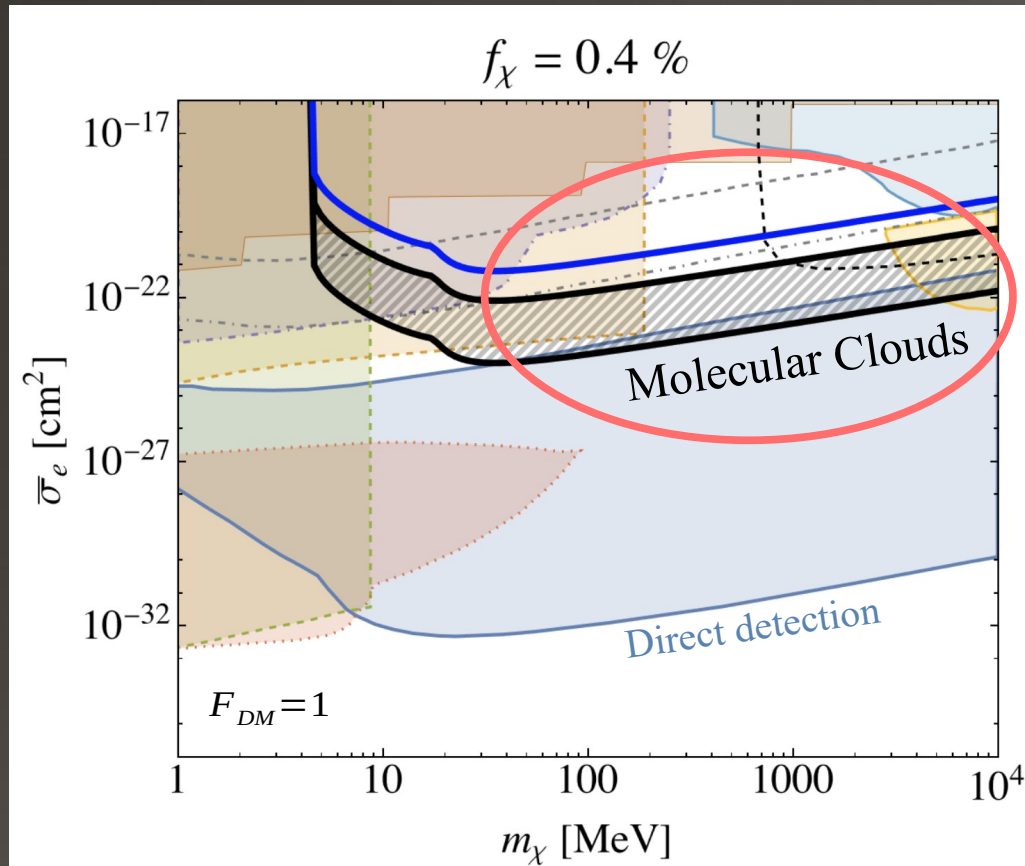


Cold molecular cloud

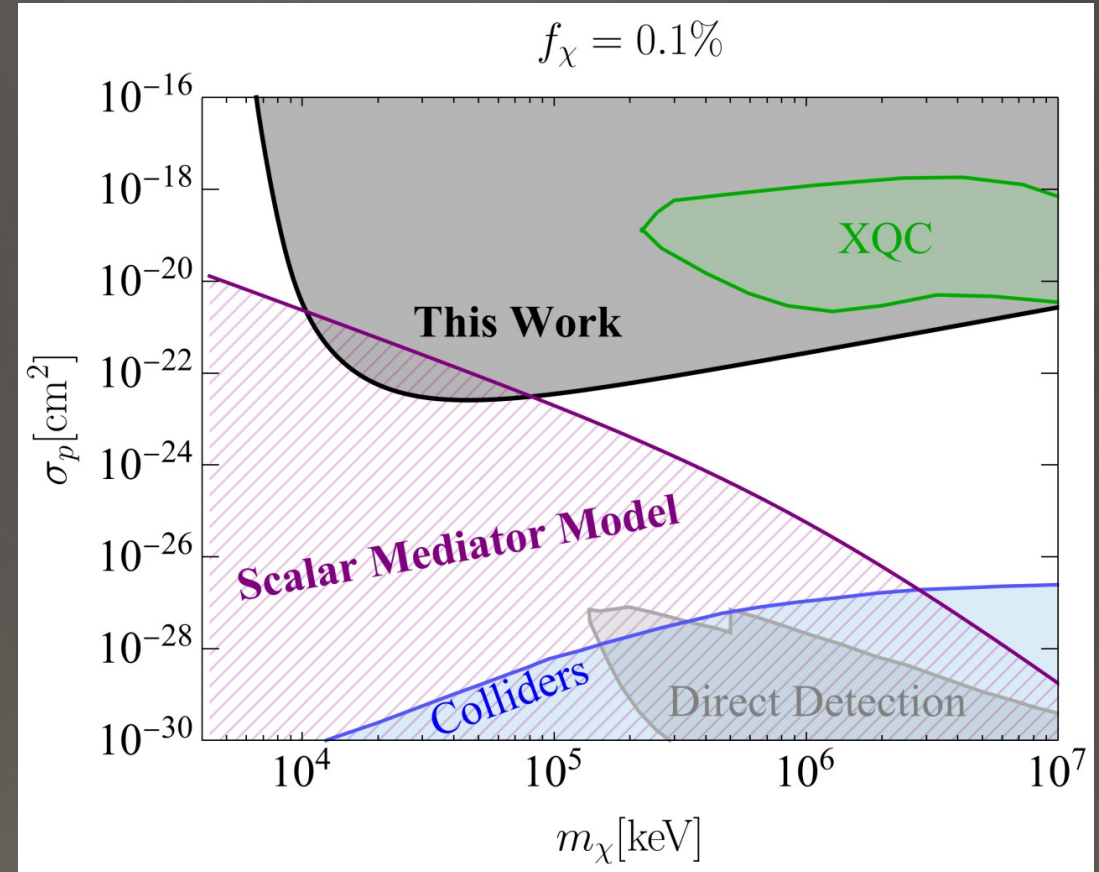


We can use the same theoretical techniques that I've developed to predict rates in detectors to predict rates in *astrophysical* objects

Dark matter in Molecular Clouds



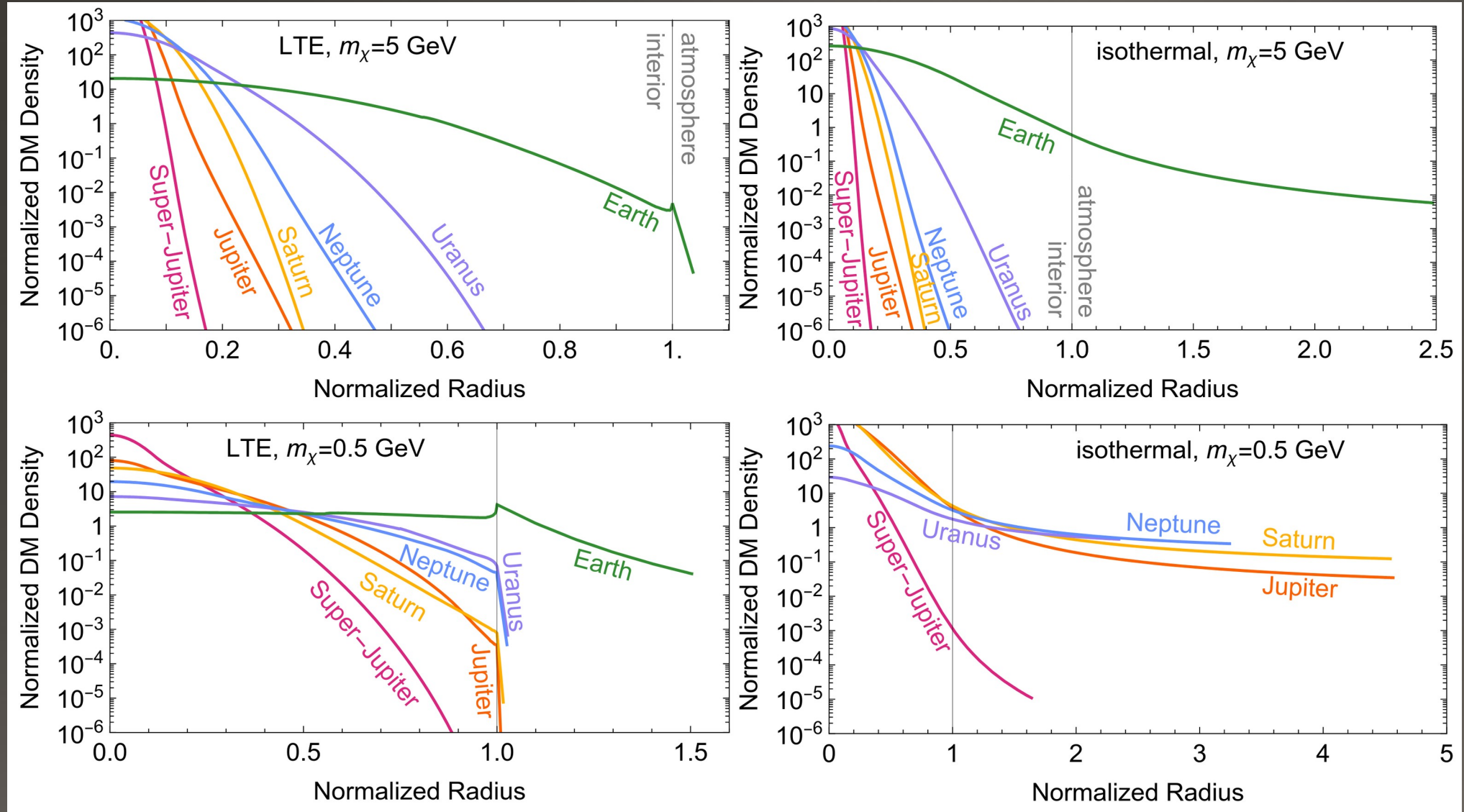
[Prabhu, CB : 2211.05787]



[CB, Harris, Kahn, Prabhu: 2310.00740]

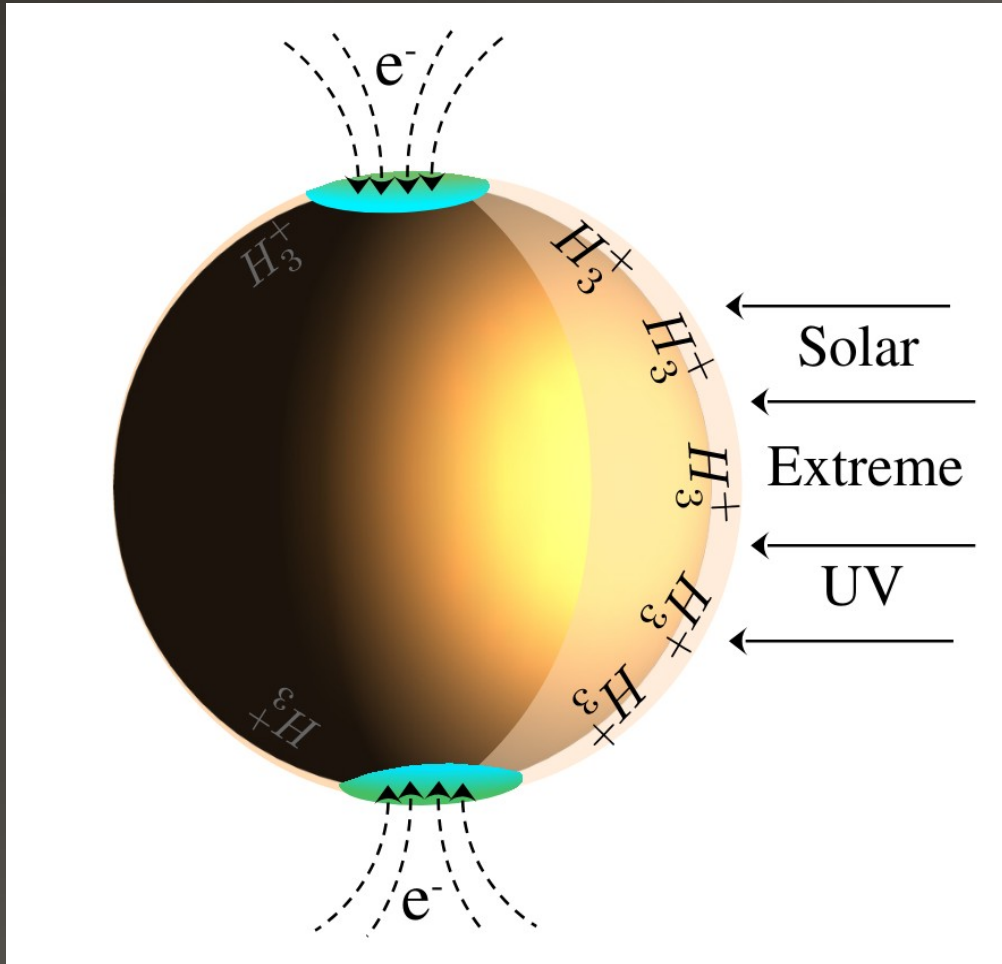
The Molecular Migdal effect(s) *in space*

Equilibrium Radial Distribution of Captured DM



[CB, Leane, Moore, Thong: 2508.00980]

IR Signatures of DM in Jupiter



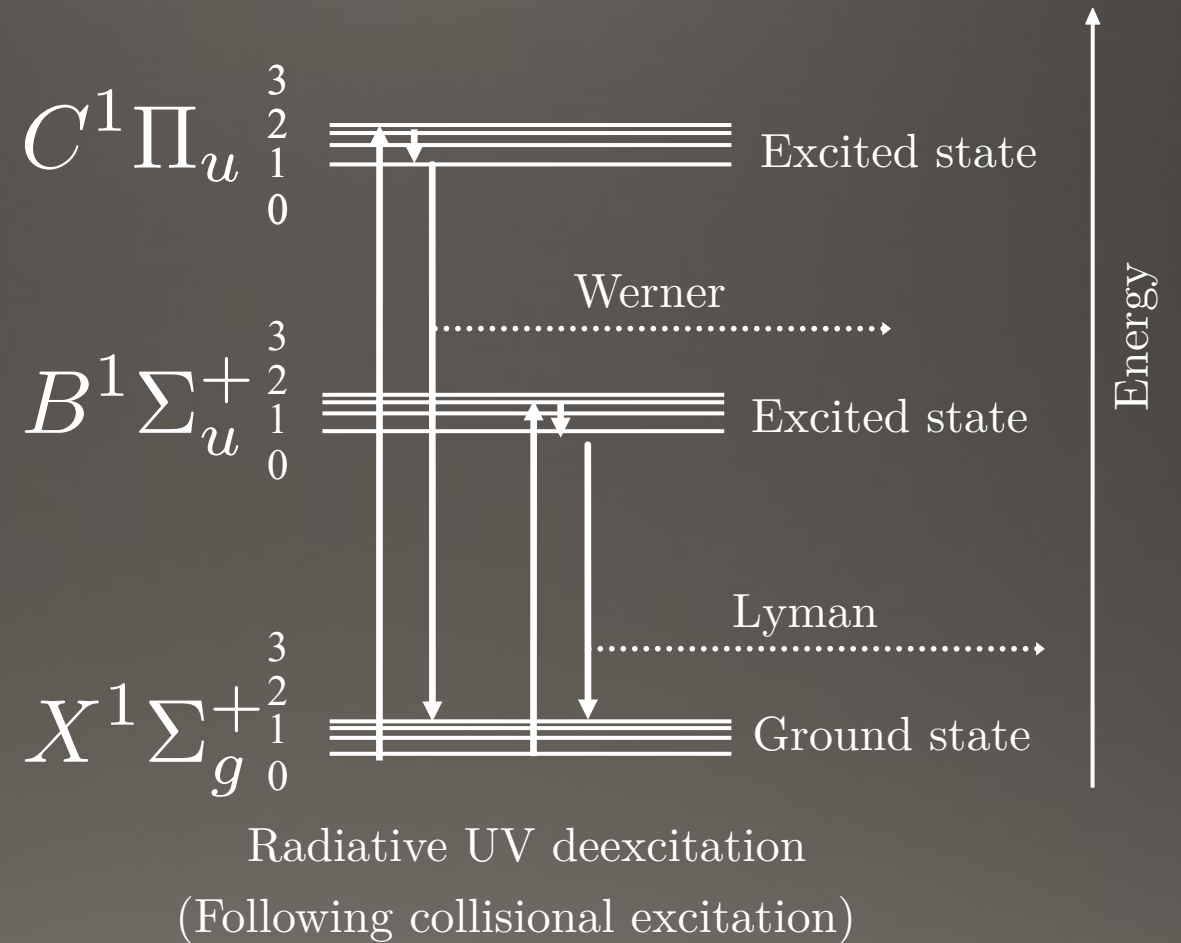
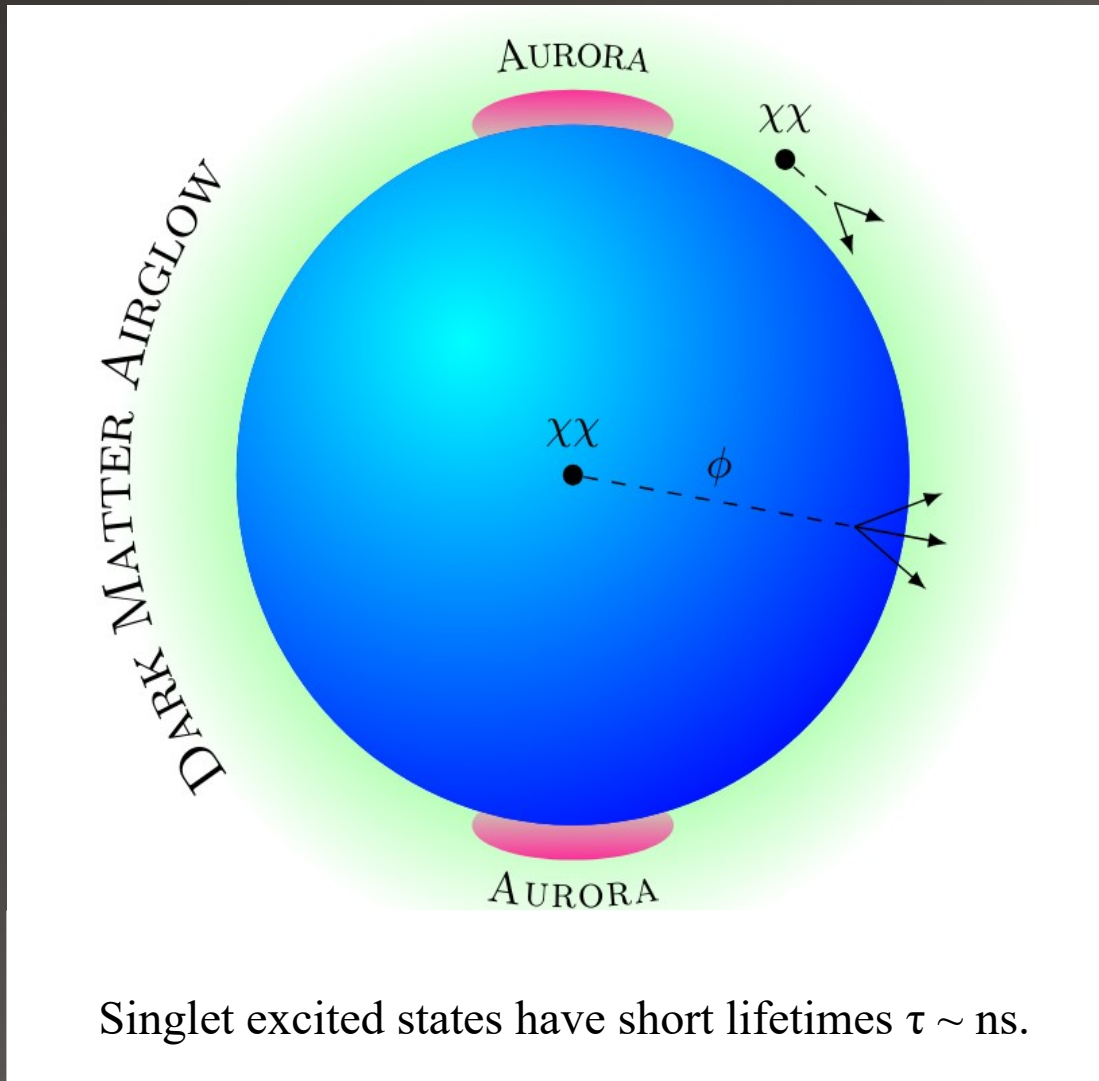
[CB, Leane: 2312.06758]

Ionizing radiation generates H_3^+

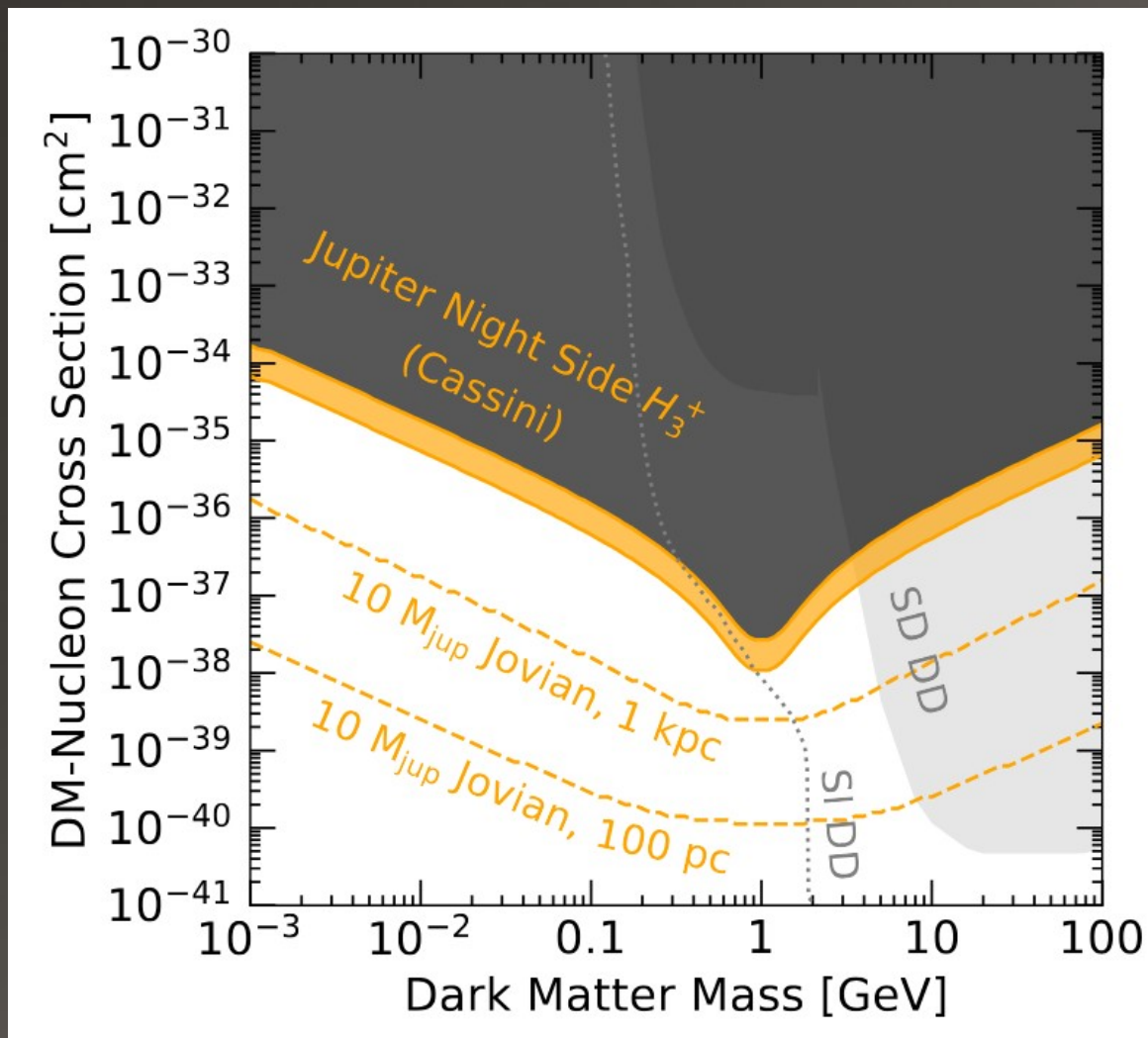
H_3^+ radiates extremely efficiently in the IR. It is Jupiter's *thermostat*.

DM Annihilation \rightarrow Brighter H_3^+ emission

UV Signatures of DM in Jupiter

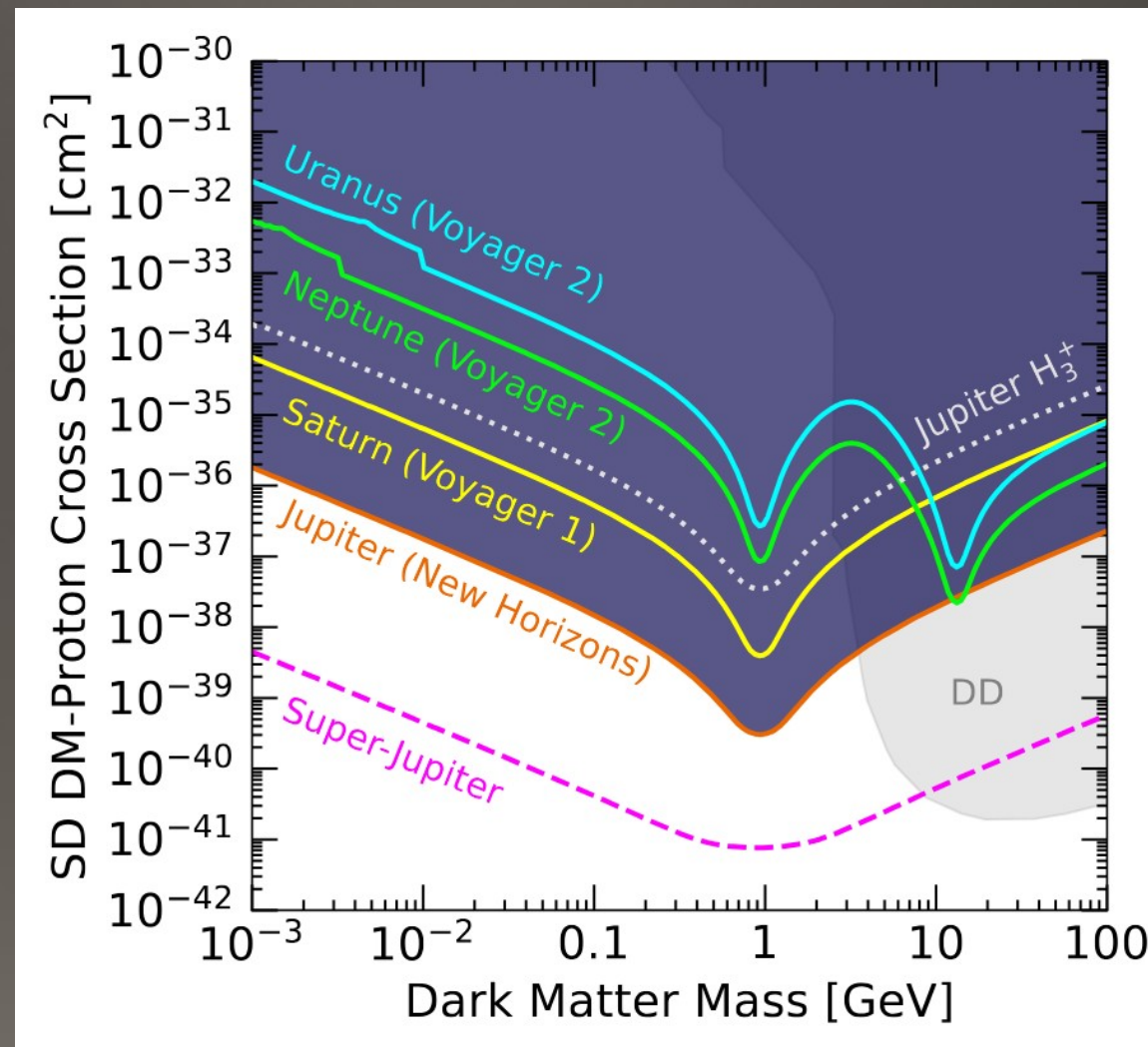


Constraints from IR and UV Molecular Emission



[CB, Leane: 2312.06758]

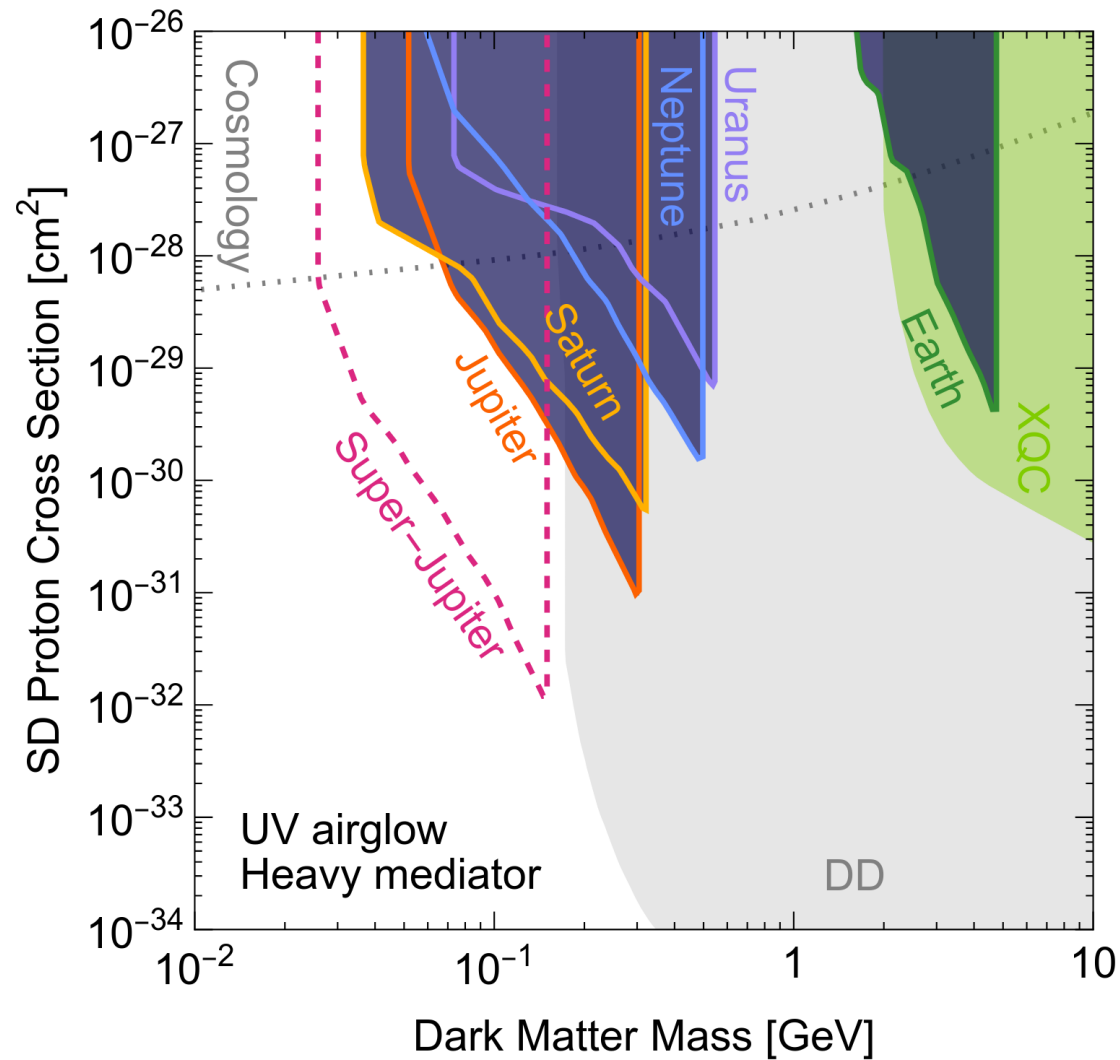
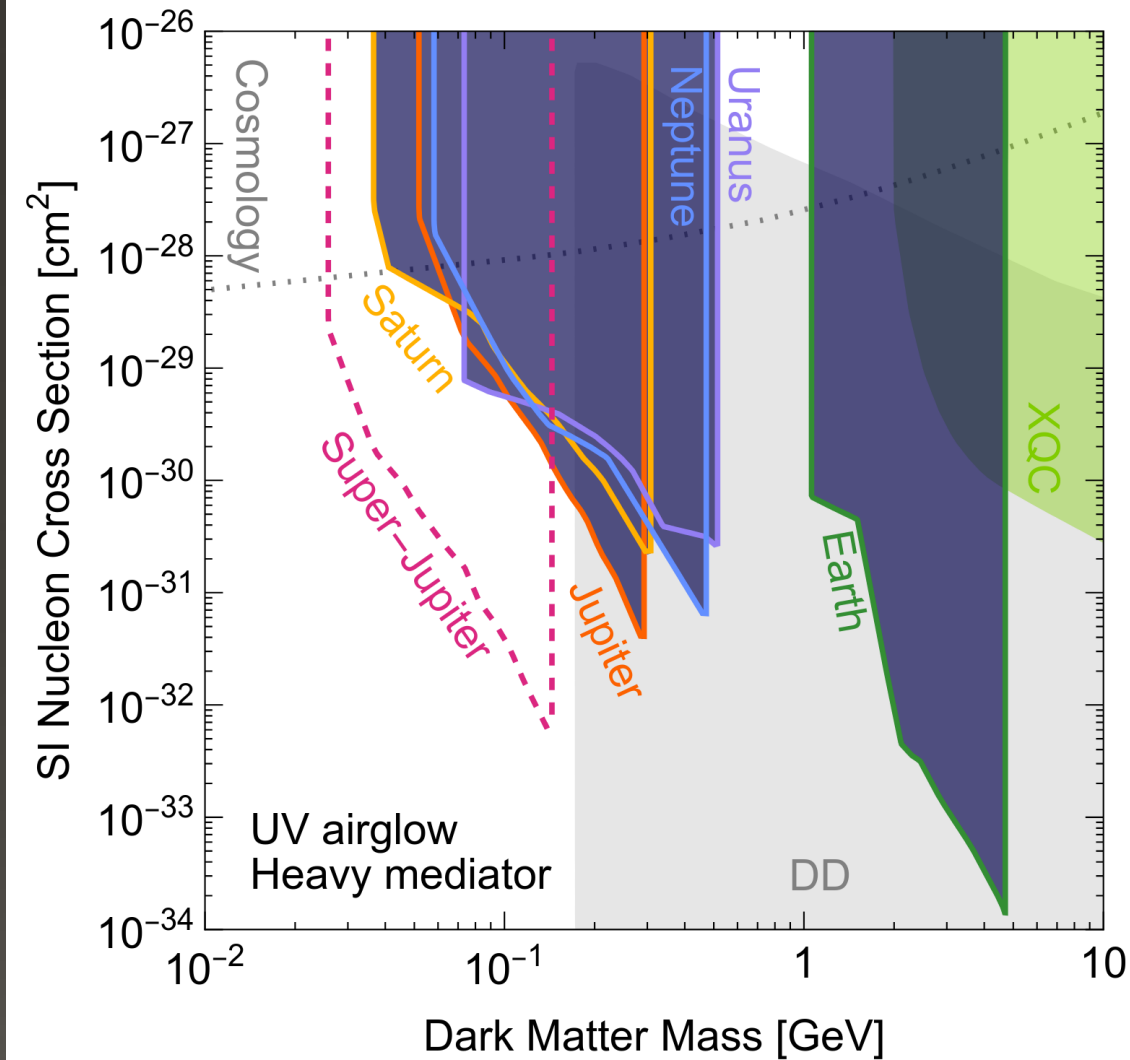
H_3^+ IR night-side emission



[CB, Leane, Moore, Thong: 2408.15318]

UV night-side airglow

Evaporation



UV airglow

[CB, Leane, Moore, Thong: 2508.00980]

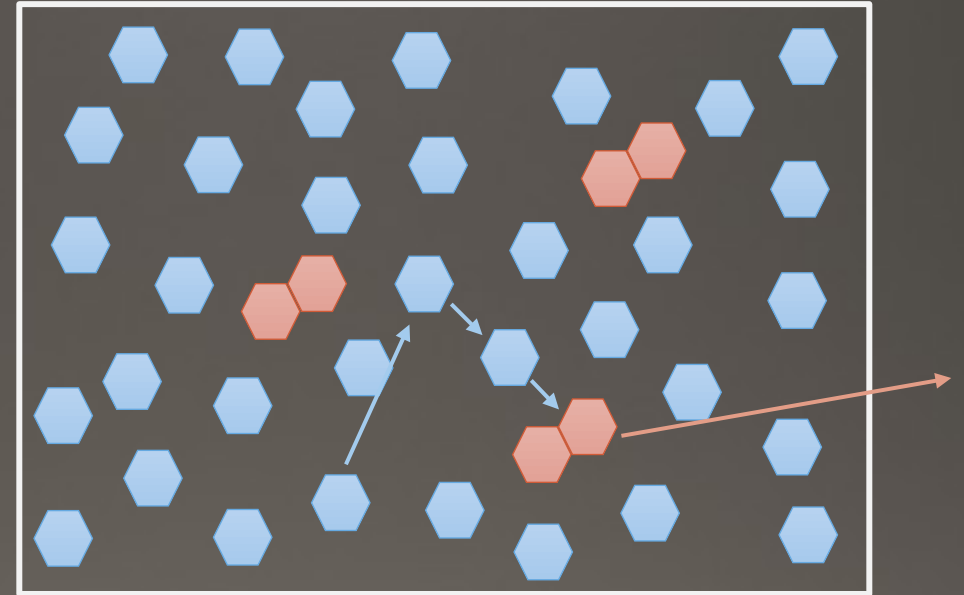
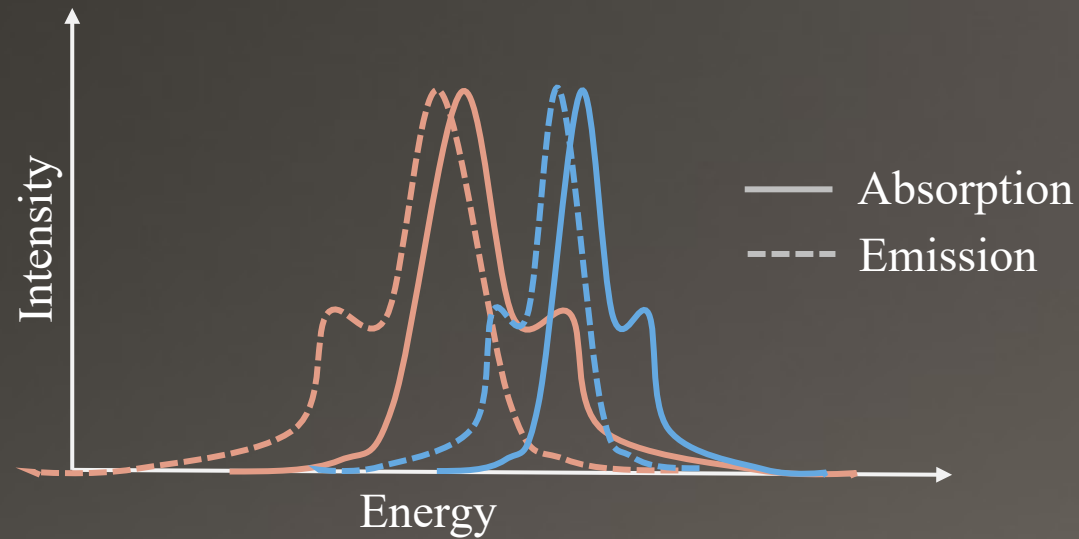
Fluorescence: Binary Scintillators



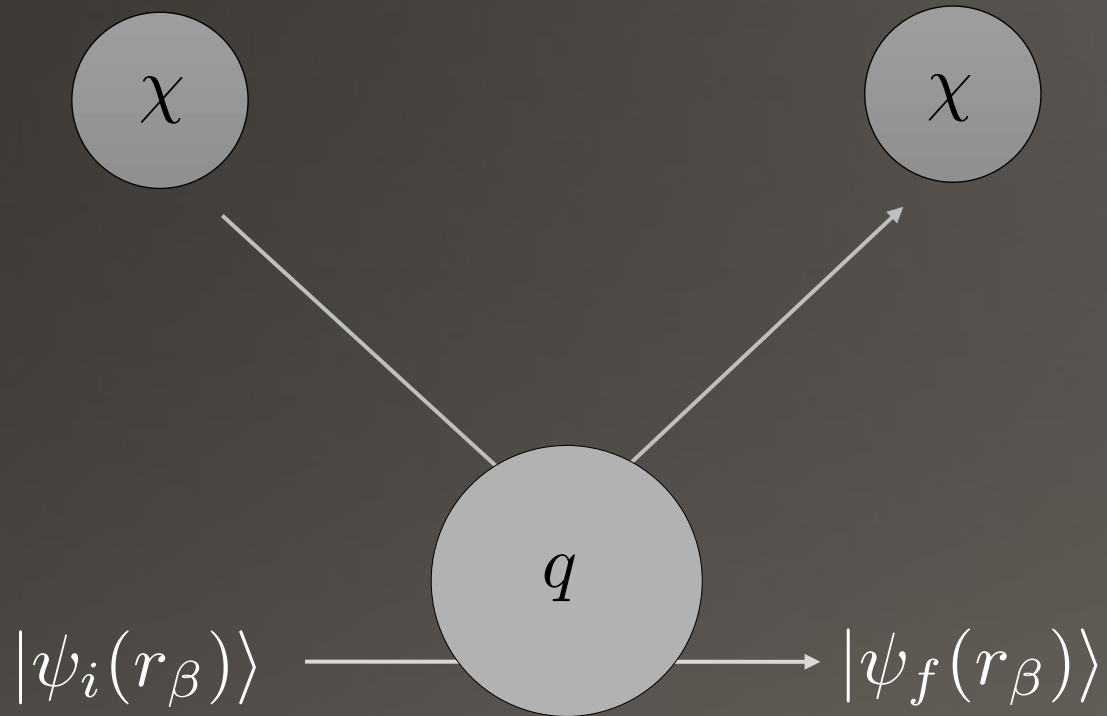
Solvent: Primary target starts the signal



Solute: Dilute fluor gets the signal out of the bulk



Electron Recoil: Charge Signal



Electron scattering

$$\Delta E_r = (m_\chi^2 / m_T) \times 10^{-6}$$

$$\Delta E \sim \mathcal{O}(\text{few eV}) \left(\frac{m_\chi}{1 \text{ MeV}} \right)^2$$

What has such transition energies?

- Semiconductor band gaps
- Maybe atomic ionization

Electrons in crystals (exciton generation)

$$|\psi_i\rangle \sim u_v(r) e^{ik' \cdot r} \quad |\psi_f\rangle \sim u_c(r) e^{ik \cdot r}$$

Electrons in atoms (ionization)

$$|\psi_i\rangle \sim \psi_{\text{STO}}(r_\beta) \quad |\psi_f\rangle \sim e^{ik \cdot r}, \quad r \gg a_0$$

Trans-Stilbene

s	Platt Symbol	Symmetry	ΔE [eV]	Configuration amplitudes			
s_1	1B	B_u	4.240	$d_{7,8} = 0.94,$	$d_{4,11} = -0.24$		
s_2	$^1G^-$	B_u	4.788	$d_{7,10} = 0.53,$	$d_{5,8} = 0.53,$	$d_{6,11} = 0.37,$	$d_{4,9} = -0.37$
s_3	$^1G^-$	A_g	4.800	$d_{7,9} = 0.53,$	$d_{6,8} = 0.53,$	$d_{5,11} = 0.37,$	$d_{4,10} = -0.37$
s_4	$^1(C, H)^+$	A_g	5.137	$d_{7,11} = 0.41,$	$d_{5,9} = -0.41,$	$d_{6,10} = -0.41,$	$d_{4,8} = -0.59$
s_5	$^1H^+$	B_u	5.791	$d_{5,10} = 0.54,$	$d_{6,9} = 0.54,$	$d_{7,12} = 0.33,$	$d_{3,8} = 0.33$
s_6	$^1G^+$	A_g	6.264	$d_{7,9} = 0.68,$	$d_{6,8} = -0.68$		
s_7	$^1C^-$	A_g	6.013	$d_{7,11} = 0.66,$	$d_{4,8} = 0.54,$		
s_8	$^1G^+$	B_u	6.439	$d_{7,10} = 0.65,$	$d_{5,8} = -0.65$		

Table 1: The first eight excited states $s_{n=1\dots 8}$, with their energy eigenvalues $\Delta E(s_n)$ with respect to the ground state and coefficients $d_{ij}^{(n)}$ as calculated by Ting and McClure.

$$|s_n\rangle = \sum_{i,j>i} d_{ij}^{(n)} |\psi_i^j\rangle,$$

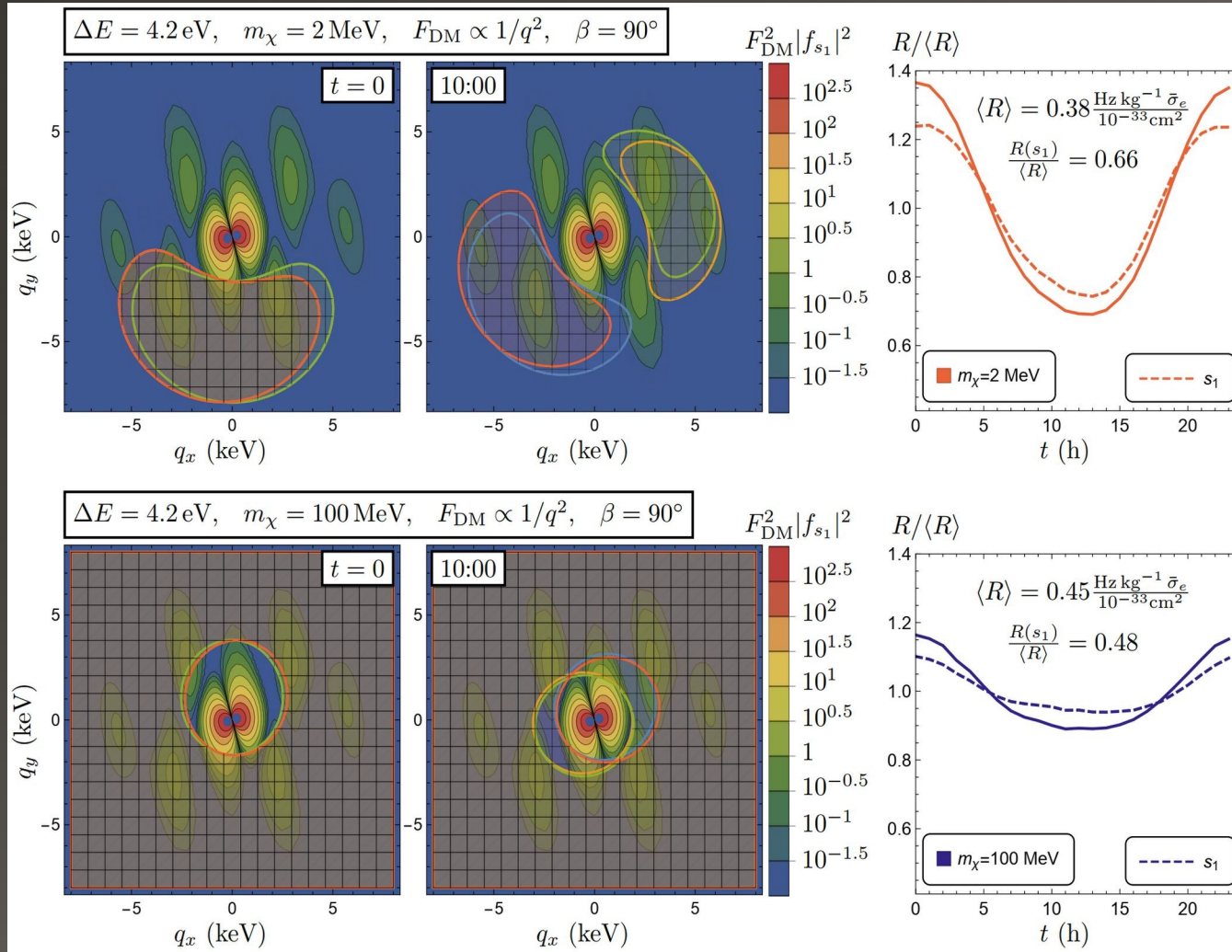
$$\sum_{ij} |d_{ij}^{(n)}|^2 = 1.$$

$$f_{g \rightarrow s_n}(\vec{q}) = \left\langle \psi_{s_n}(\vec{r}_1 \dots \vec{r}_{14}) \left| \sum_{m=1}^{14} e^{i\vec{q} \cdot \vec{r}_m} \right| \psi_G(\vec{r}_1 \dots \vec{r}_{14}) \right\rangle$$

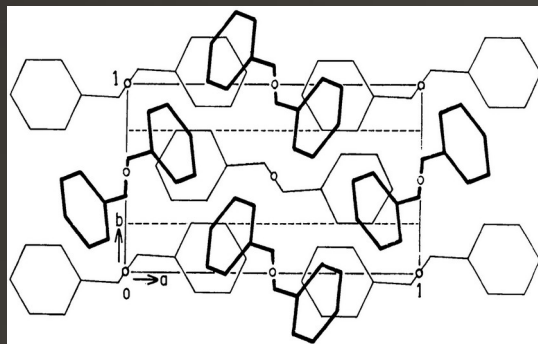
$$= \sum_{ij} d_{ij}^{(n)} \left\langle \psi_i^j | e^{i\vec{q} \cdot \vec{r}} | \psi_G \right\rangle$$

$$= \sqrt{2} \sum_{ij} d_{ij}^{(n)} \langle \Psi_j(\vec{r}) | e^{i\vec{q} \cdot \vec{r}} | \Psi_i(\vec{r}) \rangle.$$

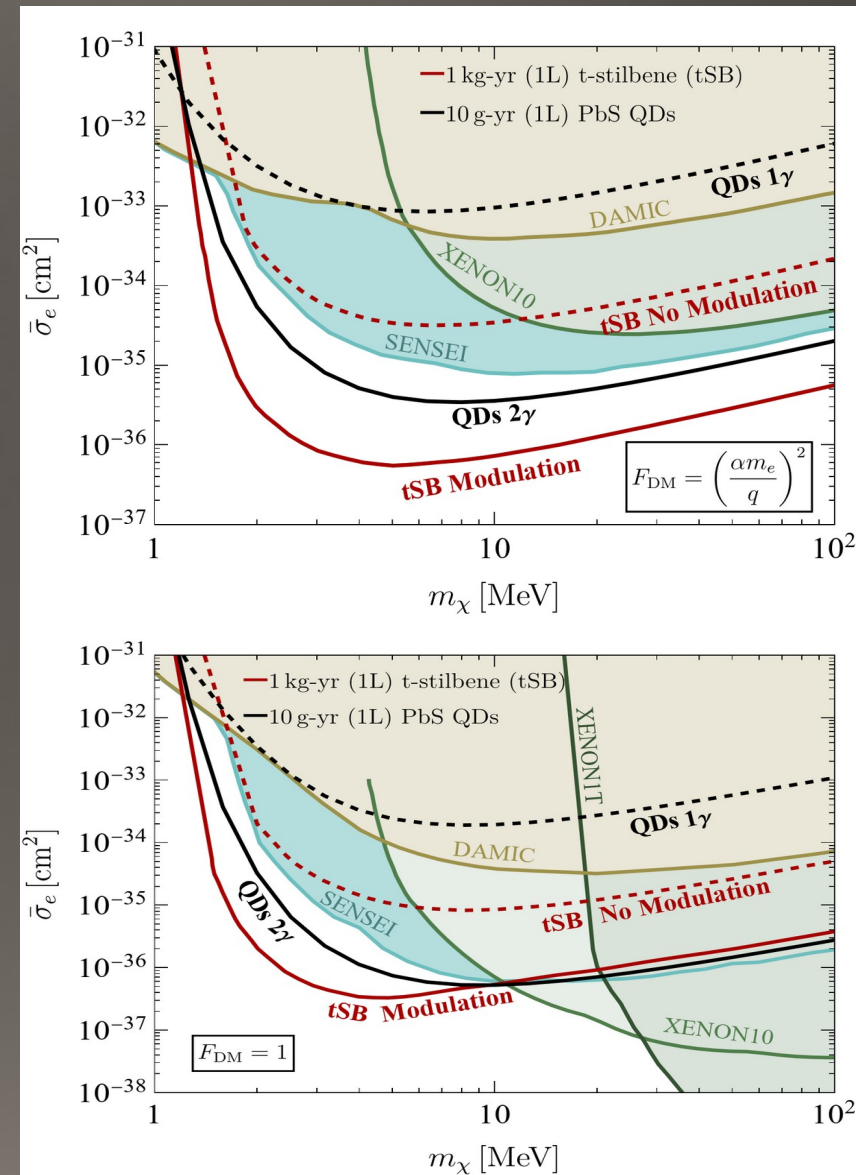
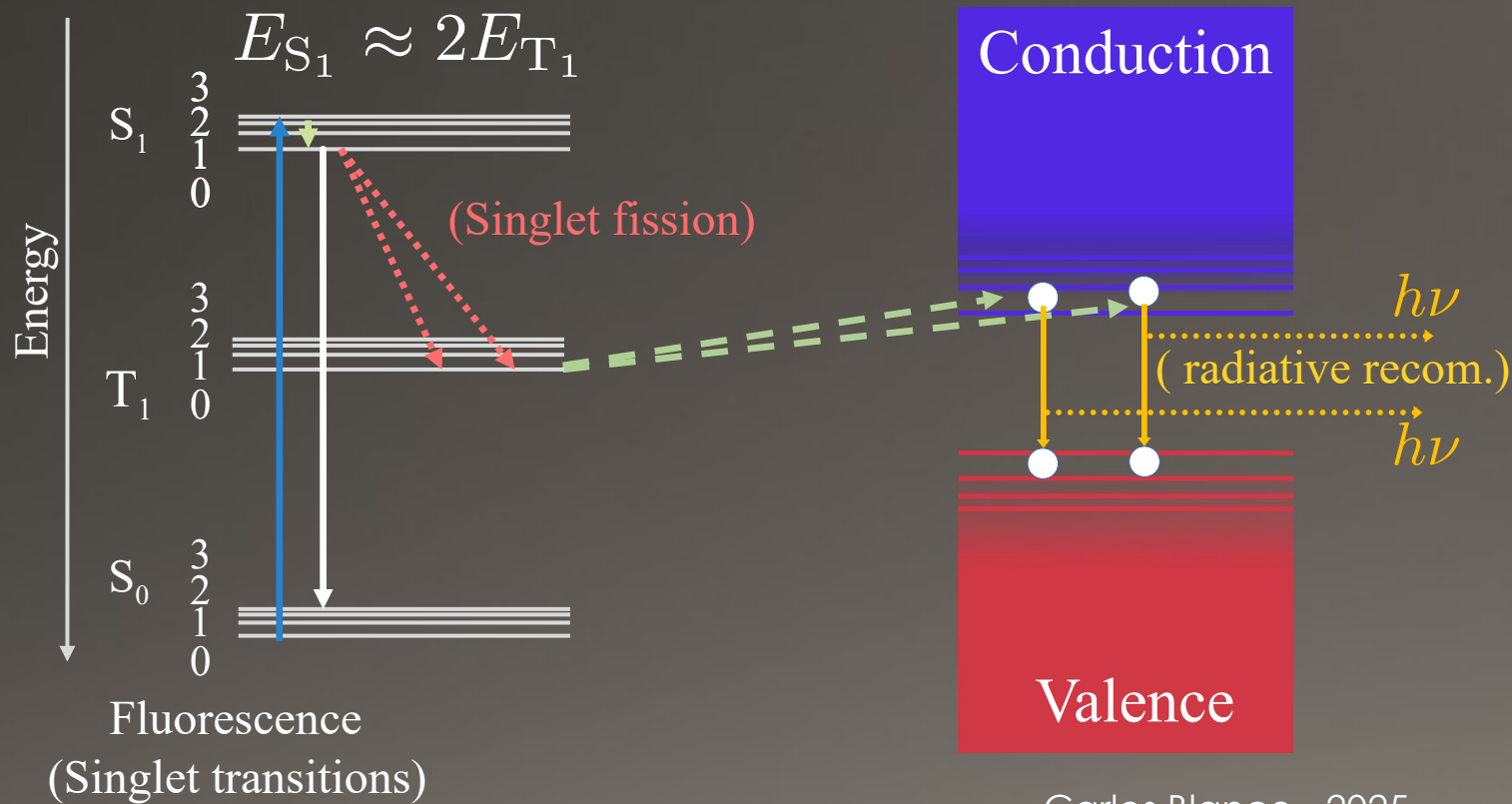
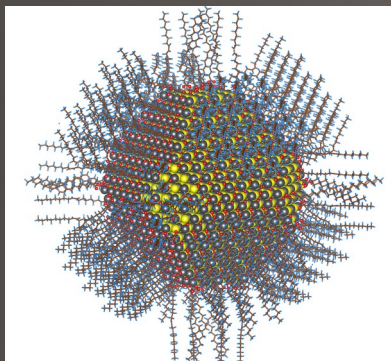
Daily Modulation: Light Mediator



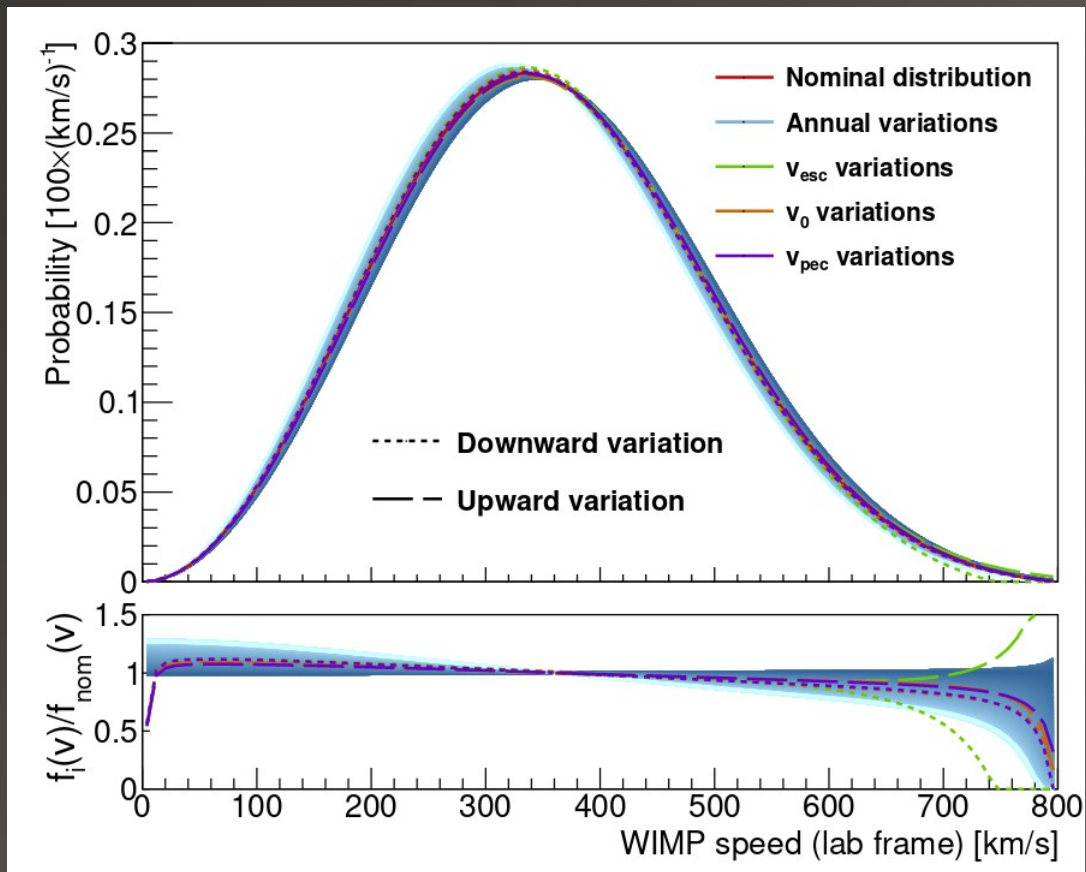
Same as previous figures (top) for a light mediator DM form factor $F_{\text{DM}} = (\alpha m_e/q)^2$. Here, the contour plots show $F_{\text{DM}}^2 |f(s_1)|^2$ which appears in the rate integrand; the scattering is dominated by the smallest kinematically-allowed q . **Top:** Molecular form factors with $q_z = 0$ and rate modulations for $m_\chi = 2 \text{ MeV}$. **Bottom:** Molecular form factors with $q_z = 0$ and rate modulations for $m_\chi = 100 \text{ MeV}$.



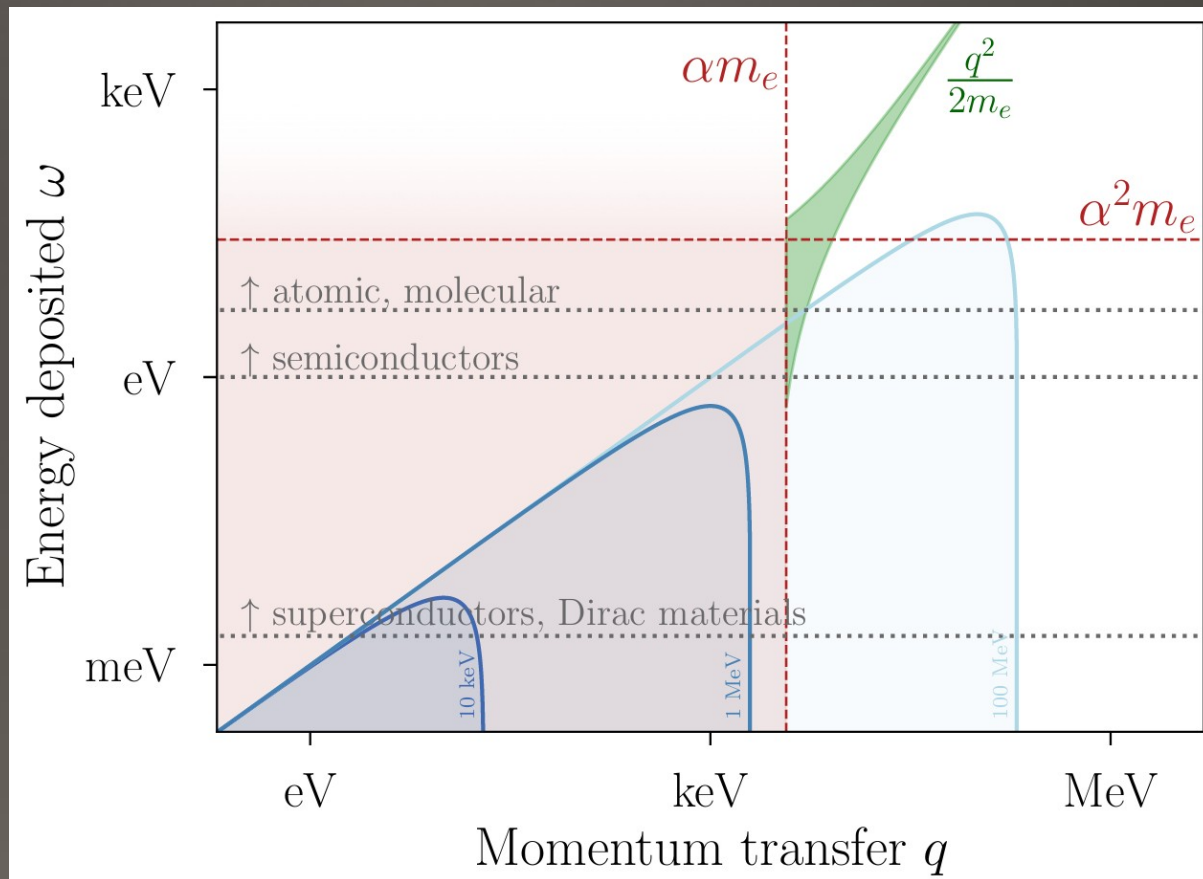
(Triplet diffusion)



Local DM Phase Space



Baxter, D., et al. "Recommended conventions for reporting results from direct dark matter searches." The European Physical Journal C 81.10 (2021): 1-19.



Lin, Tongyan. "Sub-GeV dark matter models and direct detection." SciPost Physics Lecture Notes (2022): 043.